

POLITECNICO DI TORINO

MASTER IN MECHANICAL ENGINEERING

A.Y. 2024/2025

Graduation session October 2025

Airflow study and acceptance criteria for fan testing in automotive infotainment systems

In collaboration with



Candidate: Francesco CASAVECCHIA Academic Supervisor: Prof. Federico COLOMBO

Company Supervisor: Eng. Valerio TURRIONI

Table of contents

A	bstra	t	5
1	Intr	eduction and collaboration with ART	7
	1.1	Problem	7
	1.2	Idea	8
	1.3	Collaboration with ART	10
2	Rec	nirements and Fan function	11
	2.1	Requirements	11
	2.2	State of the art	12
		2.2.1 Ultrasonic flow meters	12
		2.2.2 Thermal mass flow meters	14
		2.2.3 Differential pressure meters	15
	2.3	Fan theory and Fan function	16
		2.3.1 Technical review	17
		2.3.2 Fan and its functions	20
3	Ven	uri effect and solution	24
	3.1	Technical background	25
	3.2	Venturi design	28
	3.3	Additive manufacturing and CFD simulation	30

		3.3.1	Manufacturing process	30
		3.3.2	Air Flow simulation	33
4	Sens	sors ar	nd electronics set up	38
	4.1	Sensor	rs selection	38
		4.1.1	SDP810-500Pa	39
		4.1.2	SHT85	40
	4.2	Digita	l part and system connection	42
		4.2.1	I ² C Protocol	42
		4.2.2	Digital system connections	44
		4.2.3	Sensors identification	45
	4.3	Arduir	no Script	47
5	Dat	a acqu	uisition and testing solution	49
	5.1	Acquis	sition process	49
	5.2	System	n characterization and working point	51
	5.3	Accep	tability range for testing	54
Co	onclu	sion		57
	Futu	ıre deve	elopments	58
\mathbf{A}_{l}	ppen	dix A	Arduino code	59
$\mathbf{A}_{\mathbf{j}}$	ppen	dix B	Python code	63
Bi	bliog	graphy		65
A	cknov	wledge	ements	68

Abstract

Infotainment system is composed of many devices, the overall structure is managed by a central ECU (Electronic Control Unit). Within ECU platform development, validation and testing processes play a fundamental role in obtaining high-quality product. One of the first issues to take into account during development is heat extraction from the ECU, for that purpose a small DC axial fan is used to generate forced convection inside the box and dissipate most of the heat from the PCBs. Emerged the need to test and validate the fan cooling functions. In order to generate a testing process, the fan volumetric flow rate extracted as well as the temperature and humidity of extracted air are evaluated conveying the flow into a Venturi tube fabricated using Additive Manufacturing, performing measurements with digital sensors. CFD analysis is also carried out to compare the results with the empirical data. The target has been achieved by setting up a standard procedure to verify the correct functioning of the fan.

Chapter 1

Introduction and collaboration with ART

1.1 Problem

The ECU production and assembly process comprehends both automated and manual phases. For the second ones, the operator is in charge to assemble all the parts within the mechanical structure including also mounting process of the fan which comprises connecting cables and inserting the fan into the dedicated position inside the housing. The whole process lacks a phase in which the fan is tested to work correctly and possible problems could be related to incorrect installation, since the fan is really similar on both sides and is not always certain the correct installation by sight, which could lead to air suction problems.

Another problem is related to possible and unexpected objects obstruction to air flow, since testing environment includes many devices and staff but also papers that can accidentally fall inside the housing to hinder air extraction. In the end, even fan malfunctioning due to a manufacturing error or undetected harmful fall can occasionally occur.

The best option to ensure that air flow is enough to cool down the assembled ECU is to obtain a complete air flow characterization by measuring certain parameters to verify whether they meet or not the needed cooling capability and sell a reliable product to the customer who always expects the best performance from the product.

1.2 Idea

The first concept focuses on the development of a dedicated testing bench directly within the production plant, since in the automotive standard an automatic 100% EoL test (End of Line test) must be ensured for all functionalities of the product. This bench would allow the Electronic Control Unit (ECU) to be positioned and connected to the system for immediate testing. By simulating real operating conditions, the bench would evaluate the fan cooling function and verify the ECU's performance in a controlled environment. This solution would allow the company to have a 100% testing capability for the cooling system along with other testing processes.

The primary function of the bench would be to assess the performance of the cooling system, thus the correct functioning of the fan. By running the test based on predefined parameters, e.g. running the fan at certain speeds (rpm), the results must be verified to correspond to reference values, which could be single values or an interval of values.

This approach will lead to a fast and responsive validation, firstly avoiding defective components to be mounted and then detecting failures in the early stage of production without risk to deliver a malfunctioning product. The process would also increase the overall quality of the assembly process and, therefore, of the product itself.

In chapter 2 are discussed the requirements set by the company in relation to air

flow measurement and the realization of a test bench, in addition, the today's state of the art air flow measurement methods are presented which in this review include ultrasonic flow meters, thermal flow meters and differential pressure flow meters. To conclude the chapter, a review explaining the working principle of a fan in general is explained by then focusing on small axial DC brushless fans which relates to the fan employed for the project.

Chapter 3 is meant to clarify the reason for using a Venturi tube by presenting the fundamental equations that govern the physical evolution of the fluid inside it, essentially how pressure, velocity and other parameters vary during the flow. In addition, this chapter gives the basis for the calculation of the volumetric flow rate starting from the differential pressure value. Moreover, the Venturi tube design process is presented, which are the main issues and design constraints, as well. In the end, the 3D printing manufacturing process employed for the nozzle and all CFD simulations are visible. In this work, the terms Additive Manufacturing and 3D printing are used interchangeably, although the first is the formal designation for the fabrication process according to ISO/ASTM standard [1], 3D printing is generally used in cases of fast prototyping.

In chapter 4 the focus shifts to the electronics setup used to acquire data, and also to the sensor selection process in presented along with all the design choices. To extend the project view, a small I^2C protocol review is carried out to define the communication with the sensors. The chapter continues by showing the digital system setup selected for the project and a practical demonstration of I^2C communication by using oscilloscope acquisitions. To end the chapter, the Arduino script used for the acquisitions is presented, explaining the main code development choices and output. The final chapter 5 presents the acquisition process and the solution that has been developed in the project to produce a standardized fan testing process. In particular, the process of fan working point identification will be carried out together with

the identification of an acceptability range for fan testing that will be applied in the production line to assess the correct functioning of an ECU.

1.3 Collaboration with ART

ART was founded in the early 2000s and based in the evocative Villa del Pischiello in Passignano sul Trasimeno. Thanks to its know-how and achievements, ART is now positioned internationally as a leading manufacturer and supplier of automotive innovation and high-tech infotainment, dashboard and entertainment systems for the super sport and luxury markets. Even more recently ART has leveraged its high-level experience and expertise towards the global automotive market as well as light and heavy commercial vehicles, industrial vehicles and agricultural machinery. The company now employs more than 300 people who work at the Headquarter in Passignano sul Trasimeno and the branch offices in Modena, Turin as well as in Berlin, Germany. A flagship of Made in Italy capable of competing with the global automotive industry.

This thesis project is born from the need to provide a complete and reliable production process by verifying the correct functioning of the cooling fan, ensuring the full cooling capability of their latest and most innovative product ARTIST10.

Chapter 2

Requirements and Fan function

2.1 Requirements

The characterization of an air flow requires it to be conveyed into a defined volume in order to perform active measurement of the desired parameters such as volumetric flow rate, temperature and humidity. This chapter will clarify which are the basic requirements along with nowadays normative and technology applied to gas flow measurement and a scientific review on fan working principles and the reason why it has been chosen as thermal cooling solution for the ECU.

The test bench is required to perform the measurements autonomously, i.e. by changing the fan rotational speed, a new value of volumetric flow rate is acquired and verified to correspond to reference values. Its core requirement is to automatically calculate the mass flow rate of the fan cooling system while minimizing testing time and operator intervention, ensuring consistent and objective measurements. To reach the goal, the system would integrate specific and precise sensors and data acquisition modules that can perform a continuous measurement of the desired parameters, to then be processed in real time and analyzed to provide a clear pass/fail assessment of each ECU in short time.

Moreover, the bench would be easily accessible by the operator facilitating and reducing the amount of manual operations. This would lead to a solid and consistent procedure that enhances precision and efficiency.

2.2 State of the art

In this section a comparative review among state-of-art methods for air flow measurement is carried out. Evaluating different methods described in both the International Organization for Standardization (ISO) and the American Society for Mechanical Engineers (ASME), presenting the technologies employed, along with an analysis of their respective advantages and limitations. In particular, Ultrasonic flow meters, Thermal flow meters and differential flow meters will be described as the main options to take into account for this purpose.

2.2.1 Ultrasonic flow meters

Ultrasonic flow meters represent a non-intrusive and highly accurate class of flow measurement devices widely applied in both liquid and gas systems. Their fundamental operating principle is based on the propagation of ultrasonic waves through a flowing medium, from which the velocity of the fluid can be calculated. Two primary technologies dominate this field: transit-time (time-of-flight) and Doppler-effect-based ultrasonic flow measurement.

In the first approach, two ultrasonic transducers are installed either inline or externally on the pipe wall as shown in Figure 2.1. The transducers are capable of alternately transmitting and receiving acoustic signals both upstream and downstream of the flow. Due to the convective effect of the moving fluid, signals traveling in the direction of the flow reach the opposite transducer faster than those traveling against it. The resulting difference in transit times (Δt) is directly proportional to

the average flow velocity, and when combined with the known cross-sectional area of the conduit, enables the computation of volumetric flow rate.

In contrast, Doppler ultrasonic flow meters operate by emitting ultrasonic waves into the fluid and detecting the frequency shift of the echoes reflected by suspended particles or gas bubbles. The magnitude of the Doppler shift is proportional to the velocity of the scattering particles, and consequently to the bulk flow velocity. Doppler devices are particularly suited to applications involving multiphase fluids or contaminated media, whereas transit-time meters achieve the highest accuracy in clean, single-phase fluids such as natural gas or dry compressed air.

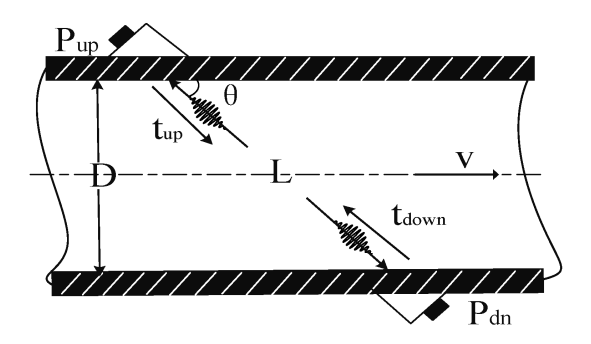


Fig. 2.1: Ultrasonic Flow Meter. Shows transducers placement on the conduit and sound waves transmission path

In the context of gas flow measurement, ultrasonic flow meters offer several compelling advantages. Their clamp-on or inline configurations eliminate intrusive components within the flow path, thereby minimizing pressure losses and mechanical degradation, which is critical in high-pressure gas pipelines and industrial process systems. Furthermore, advanced configurations using multi-path geometries (V, W, or Z arrangements) allow the measurement of multiple velocity profiles, improving the accuracy in the presence of asymmetric flow fields, swirl, or upstream disturbances. Modern ultrasonic gas flow meters can achieve accuracies of $\pm 0.5\%$ or better under proper installation and calibration conditions, while also supporting a broad range of flow rates and pipe diameters. To ensure reliable operation in

gas applications, engineers must account for factors such as low-density acoustic signal attenuation, environmental noise, and moisture or particulate contamination that may affect transit-time signal quality. Overall, ultrasonic flow metering technology has matured into a reliable solution for high-accuracy, maintenance-free gas flow measurement in both industrial and energy management contexts, offering a balance of precision, flexibility, and operational efficiency [2].

2.2.2 Thermal mass flow meters

Thermal Flow measurement is performed using a system composed of a hot wire and two temperature sensors. The principle of operation is described in Figure 2.2 below and explains how the sensors are placed in relation to the position of the hot wire component. The principle is to convey the fluid flow through an heated element

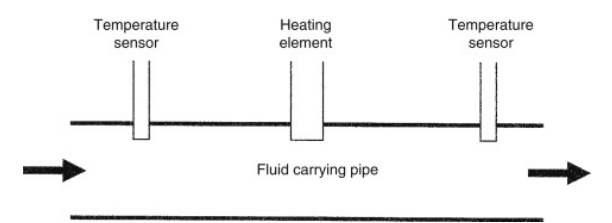


Fig. 2.2: Thermal flow meter principle of operation. Sketches the placement order of the two sensors with respect to the hot wire [3]

and measure the temperature upstream and downstream of the wire to quantify the heat loss due to the flowing fluid. Then the process of measuring the mass flow rate is carried out in two possible ways: either by measuring the temperature rise in the flowing material or by measuring the heater power required to achieve a constant set temperature difference in the flowing material. In both cases the fluid parameters such as specific heat and density can vary with temperature and pressure however these variations are typically small in most applications. In these applications where the thermal properties of the fluid are known and relatively constant during actual operation, thermal flow meters can be used to measure the mass flow of the fluid

because the thermal flow measurement is not dependent upon the pressure or temperature of the fluid. Innovation has been made among those types of flow meters introducing MEMS technology, these have the same basic structure as shown in Figure 2.2, but of course the heater and temperature sensors are both micro-electrical mechanical systems (MEMS) scale and contained within a tiny package.

Thermal flow meters provide fast response time, high accuracy, low pressure drop across the device, very low power consumption, and high reliability due to the absence of moving parts. They are well suited for stack flow measurement and emissions monitoring uses. In general, this type of technology can be employed within a wide range of flow rates from units of nanoliters per minute to the magnitude of 100L per minute. [3] [4]

2.2.3 Differential pressure meters

Differential pressure (DP) meters use Bernoulli equation as working principle to measure the fluid flow within a pipe. It is one of the most used methods and has a broad and established standardization. DP meters introduce an obstruction into a flowing fluid pipe such as orifice plates, nozzles, Venturi tubes and Dall tube as shown in Figure 2.3, that increases fluid velocity in the constriction causing a drop of static pressure.

By measuring the differential pressure (ΔP) across the obstruction, the amount of flow rate can be calculated. The higher the flow rate of the fluid inside the pipe, the higher is the ΔP measured by the device, the relation between the two quantities is quadratic and the general expression is also standardized by the ASME and ISO normatives. This kind of solution is mechanically simple and does not require a strong investment, it is characterized by high robustness and low maintenance. However, one significant disadvantage of this method is that the obstruction causes a permanent loss of pressure in the flowing fluid. The magnitude of this loss depends on the type of obstruction element used, but where the pressure loss is large, it is sometimes necessary to recover the lost pressure by an auxiliary pump further down the flow line. This technology is widely used and applied in many fields and

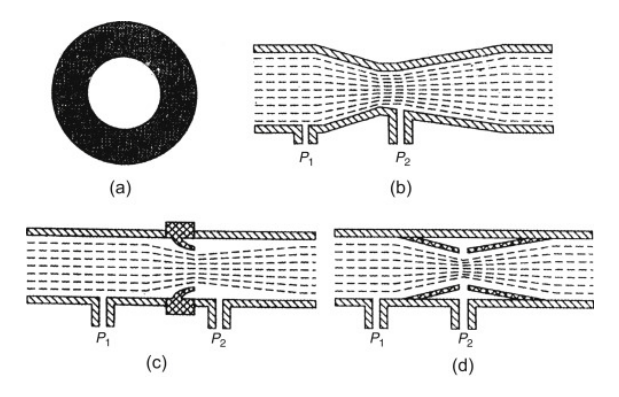


Fig. 2.3: Obstruction solutions for differential pressure meters. (a) Orifice plate; (b) Venturi; (c) Flow nozzle; (d) Dall flow tube. [3]

remains one of the most used among gas flow measurement solutions, for example, in HVAC systems but also in oil and gas industry. This solution is considered to be the most suitable for this project requirements and the most simple to realize in the context. Despite some disadvantages, it allows to satisfy the needs without consistent investment and decent accuracy. [3] [5]

2.3 Fan theory and Fan function

Fans are a widely used class of turbomachines employed for air recirculation and cooling systems, they provide energy to the fluid through a power-driven rotating impeller in order to produce air flow or pressure rise [6]. As mentioned earlier in the introduction they play a crucial role in the field of ventilation and cooling solution starting from our personal computer small fans to large ventilation fans inserted in tunnels to enhance air recirculation.

In particular the review focuses on axial fans which are related to our work. Axial

fans are devices that generate air flow parallel to the impeller rotation axis. The general structure is usually composed of a rotating part (rotor) and a static part (stator), which will be inspected more in detail in the next section. The main focus will be on small axial fans which generate a modest pressure rise and volumetric flow rate, the size together with the performances allow it to be applied as cooling source in small electronic devices such as ECUs.

2.3.1 Technical review

The principal purpose of small axial fans is to impart kinetic energy to the fluid (air in this case) to generate a flow. In essence, these widely used fans are simply single-stage compressors with a low pressure rise, that allows to provide enough energy to move the air and extract heat. Pressure is increased as a result of the rotation of an impeller driven usually by a brushless DC engine, which has accurately oriented blades that allow to transmit the kinetic energy of the blades to the air, increasing its velocity and pressure. The relation between pressure and velocity (or volumetric flow rate, Q) is quadratic inversely proportional as defined by the Fan Laws (Figure 2.4) that govern all the variable relations for the fans, the deduction obtained is that the higher the air velocity, the lower is air static pressure (SP). Further in the section will be delighted this relation by showing off the Fan curve.

$$FAN \ LAW \ 1 \qquad FAN \ LAW \ 2 \qquad FAN \ LAW \ 3$$

$$CFM_2 = CFM_1 \times \left(\frac{RPM_2}{RPM_1}\right) \qquad SP_2 = SP_1 \times \left(\frac{RPM_2}{RPM_1}\right)^2 \qquad HP_2 = HP_1 \times \left(\frac{RPM_2}{RPM_1}\right)^3$$

Fig. 2.4: Fan Laws. In the picture are shown the three fan laws that link flow rate value, static pressure and power to the fan rotational speed [7]

As mentioned before, the impeller blades and the stator ones too, are designed with a precise orientation with respect to the direction of the air flow. Firstly, rotor blades play the most important role in transmitting energy to the air since their rotation satisfies the main purpose of generating an air flow. The way in which the blades exchange energy with the air can be shown through the velocity triangle (Figure 2.5), where we can see how the air flow is guided through them. In particular we must consider the configuration on the right which corresponds to our fan structure, it may be noted how the absolute fluid velocity (c_i) is increased and canalized at the exit of the stator blades stack, thanks to the rotational speed of the rotor (tangential direction, u), absolute velocity of the fluid increases from c_1 to c_2 at the exit of the blade and then the stator allows to straighten its direction to axial to avoid losses caused by vortex generation.

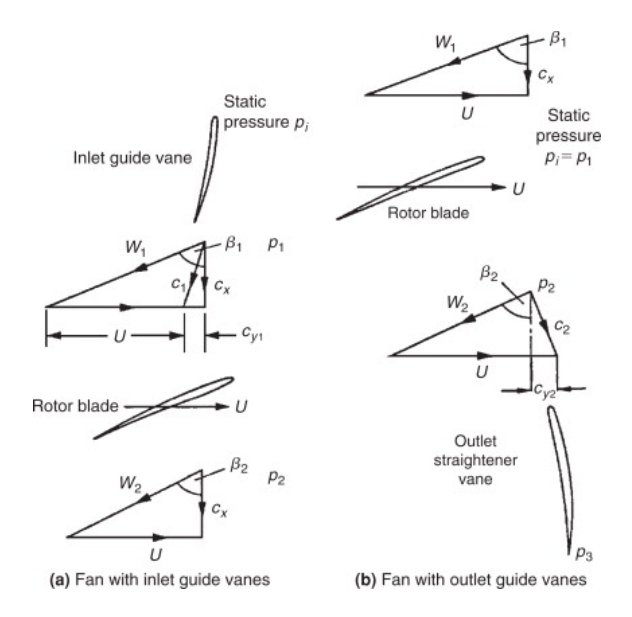


Fig. 2.5: Fan velocity triangles. (a) shows a structure in which the fluid goes through stator blades by then entering the rotor section, (b) opposite disposition of rotor and stator. [8]

In other words, the work done on the fluid by the impeller torque adds a rotational component to the velocity. As a result the absolute velocity at the exit is higher than the axial velocity, thus some of the total pressure that was developed by the fan does not appear as useful total pressure.

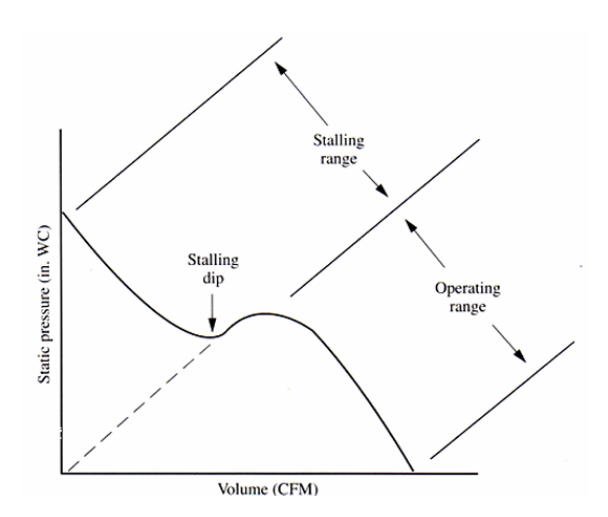


Fig. 2.6: Fan performance curve [9]

Figure 2.6 shows a general kind of fan performance curve, it starts from the point of free delivery (static pressure=0). When a restriction to the flowing fluid occurs due to a change in the environment or ducting system where the fan operates, the static pressure increases and the volume flow decreases. This is due to the fact that with increasing flow restrictions, the volume flow will decrease and the axial velocity will decrease since this velocity component is related to flow rate as we can see in Equation 2.1

$$Q = c_x \cdot A \tag{2.1}$$

The inlet angle (β in fig.2.5) of the relative velocity will increase (same rotational speed u and lower axial velocity c_x) and the angle of attack will increase and as a result the static pressure will increase (operating range). However this will happen until the maximum useful angle of attack when the peak of static pressure is reached. After that point, the angle of attack will increase above the stall point of the blade, the flow will not be able to follow the contour of the blade, separation will occur and the static pressure will finally decrease simultaneously with the volume flow (stall dip region). After the stalling dip region it would be expected that the lift coefficient will decrease until the point of zero flow and zero static pressure is reached (dashed

line). However, the fan continues its operation with low efficiency and high noise. When the fan operates in a stalled condition the flow is to some extent thrown outwards by centrifugal force and in this way static pressure is produced until the point of zero flow. [9]

2.3.2 Fan and its functions

Here follows a brief presentation of the fan employed by the company, on which the work is carried out. A concise explanation of its characteristics and advantages are underlined.

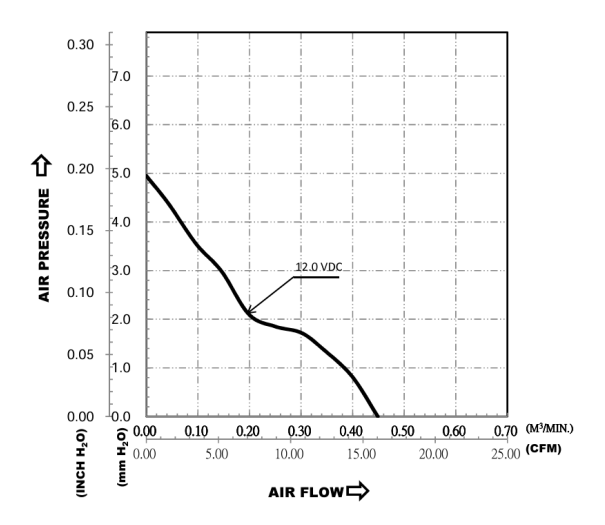


Fig. 2.7: Delta Fan Performance Curve [10]

The fan employed for the project is a Delta DC fan (Model: ASB0512MBEHD) with dimension $50X50X15 \ mm$ (Fig.2.8) supplied with 12V can reach a maximum rotational speed of $5500\pm15\% \ rpm$, capable of providing a maximum air flow of $0.450 \ m^3/min$ in the zero static pressure condition until reaching a maximum static pressure of $4.85 \ mmH_20$ with absence of air flow (those values can be seen in Fig. 2.7). By comparing Fig. 2.6 and Fig. 2.7 we can notice that there is not a clear separation between the stall region and the operating range in the Delta curve, which

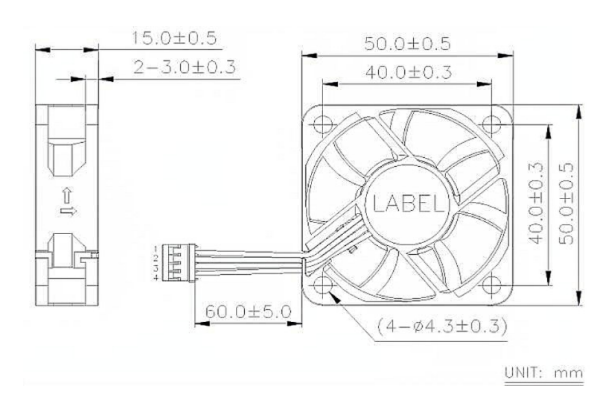


Fig. 2.8: Fan technical drawing. Shows the dimensions and configuration of the fan [10]

allows to avoid the stall of the blades and obtain a broader interval to operate the fan. In addition, the image of the Delta fan curve is referred to an operational speed of 5500 rpm that corresponds to a maximum air flow condition, which is an unusual operating condition, later in the section a complete curve showing the operation at different speeds is presented (Figure 2.9). As we expected by considering the theoretical review made above, the relation between volumetric air flow and static pressure is inversely proportional, not many considerations about blades angle are clarified in the datasheet so we cannot make a technical comparison about it. [10] The communication between the ECU and the fan is governed by a PWM (Pulse Width Modulation) technique, in fact in Fig. 2.8 is visible the wiring composed of four wires that are typical for PWM control. The working principle is related to the Duty Cycle (DC) variation, essentially the ECU controls the speed of the fan by changing the DC, the higher the DC the higher is the fan speed.

The duty cycle is a measure of the fraction of time a signal, device, or system is active (ON) compared to the total cycle time, in our case a 100% DC corresponds to a speed of 5500rpm and for a 0% duty cycle the fan is off, while for values of DC in the middle there is a full range of speeds possible. In practice, for values of DC under 30% the energy is not enough to move the fan, therefore to start the rotation, a DC above that value is needed, Fig. 2.9 shows some of the speeds related

to different duty cycle values. This graph will help to investigate the working point of the fan and then generate a standard and solid testing process.

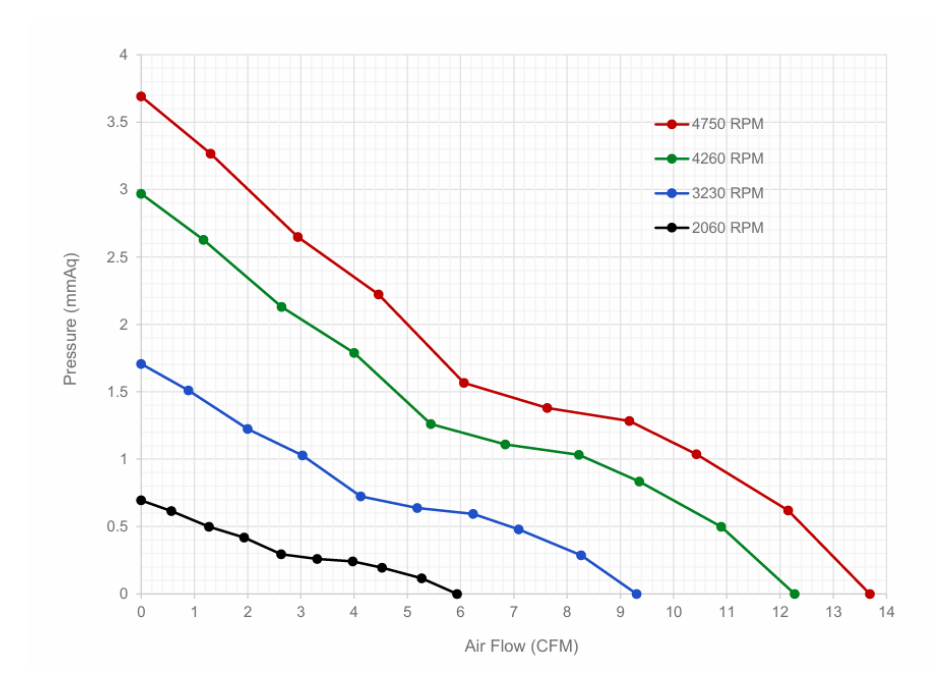
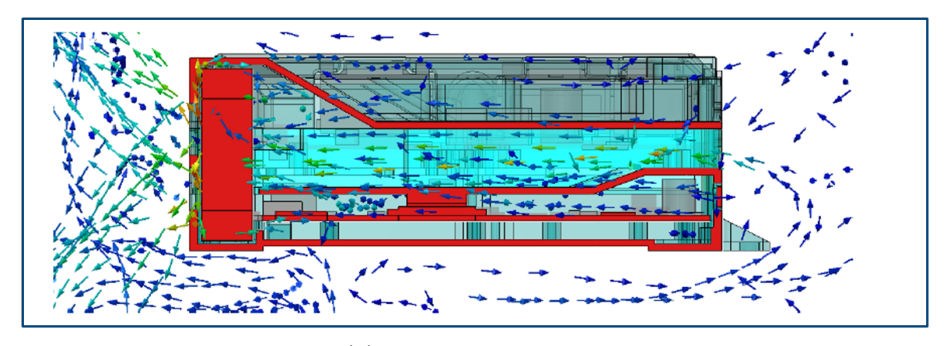


Fig. 2.9: Delta fan curve parametrized at different speeds. Each speed in the graph correspond to a certain value of Duty Cycle. [10]

The fundamental role of the fan is to produce forced convection inside the ECU environment to help thermal management cooperating with already existing heat conduction in order to guarantee Automotive standard compliance of temperature limitation to electronic components under 105°C [[11], [12]] and make sure a working life of the components of at least 15 years. In Figure 2.10 is shown the simulation carried out by the company, in which are visible the flux vectors of the air that passes through the different components of the PCBs and cooling down all the whole environment managing to reach even narrow spaces. The critical components, marked as red in the picture, need advanced thermal management with optimized heat extraction achieved by directly coupling the components to the housing through special materials that expand when heated, thereby increasing the contact surface and enhancing conduction.



(a) View from the side

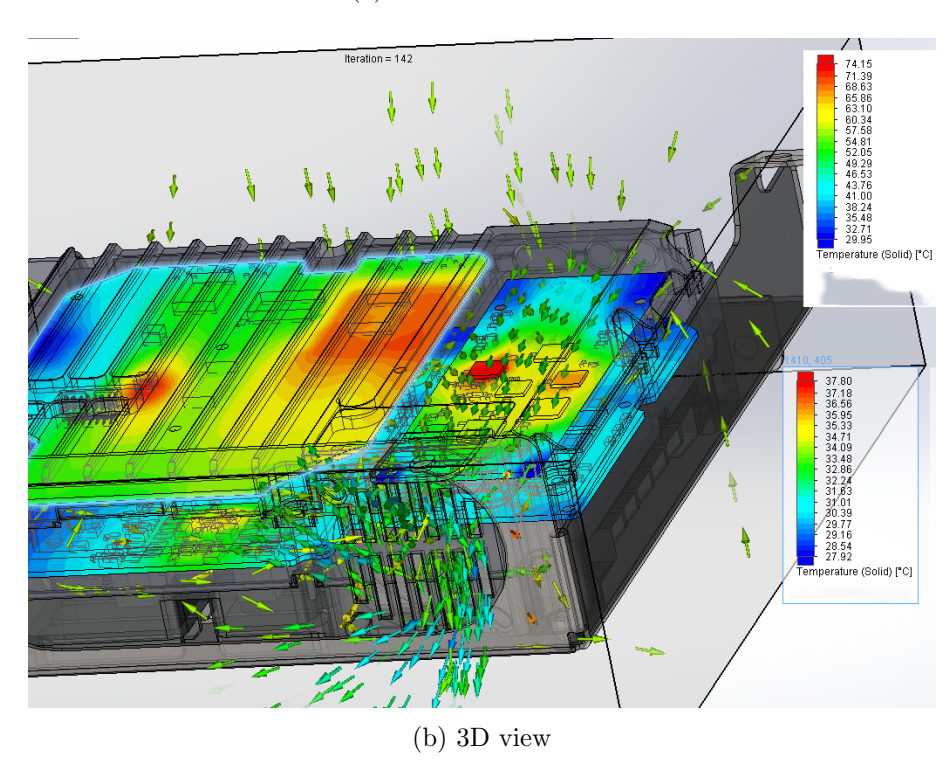


Fig. 2.10: In figure (a) is possible to see the side of the ECU and how the air flux is moved by the fan. In figure (b) the 3D view allow to see which are the hotter components and how the air flux is canalized through them.

Chapter 3

Venturi effect and solution

The solution and satisfaction of the requirements is based upon Venturi effect which derives from Bernoulli's principle (Eq.3.1) and takes advantage of mass flow rate conservation.

$$H = z + \frac{p}{\gamma} + \frac{v^2}{2q} \tag{3.1}$$

The effect is the reduction in static pressure that occurs when a fluid flows through a constricted section, or "throat," of a pipe, as the fluid enters the narrow section, its velocity increases to maintain a constant volumetric flow rate (conservation of Equation 2.1). This principle is fundamental in many applications, from carburetors that mix fuel and air in engines to Venturi meters used to accurately measure the flow rate of liquids and gases in industrial pipelines. The project consists of the design and application of a Venturi meter, the specific feature is that the air never changes its elevation head z referring to Equation 3.1 during the flow, therefore, the only changing parameters are static pressure p and air speed v, which allow to measure the volumetric flow rate due to their variation.

3.1 Technical background

In this section a thermo-fluid-dynamic analysis is carried out, with the aim of providing an empirical description of the air flow inside the Venturi, in order to have a theoretical acknowledgment on how physical parameters evolve during the flow (such as pressure, temperature and speed). Continuity equation (or mass conservation equation, 3.2) and energy conservation equation will be analyzed to reach the scope:

$$\frac{\delta\rho}{\delta t} + \nabla \cdot (\rho \vec{v}) = 0 \tag{3.2}$$

where ρ is air density and \vec{v} is a velocity field in space, this is the local expression of the equation above, which is a stronger condition with respect to a general expression. In the same form is written the energy conservation equation considering an infinitesimal volume dV of fluid:

$$\delta \dot{Q} - \delta \dot{W} - \frac{\partial (pu_i)}{\partial x_i} = \frac{\partial}{\partial t} \rho \left(e + \frac{u^2}{2} + \rho gz \right) dV + \frac{\partial}{\partial x_i} \left[(\rho u_i) \left(e + \frac{u^2}{2} + \rho gz \right) \right] dV$$
(3.3)

here we can see a complete version of the energy conservation equation, where u is the fluid speed, e is the internal energy, $\delta \dot{Q}$ and $\delta \dot{W}$ are respectively the heat transfer rate and the rate of work done across the meter.

Considering those two equations now, some hypotheses related to this case are applied. Firstly, the system can be assumed to have no heat transfer and no work being done across it, along with steady-state conditions. Then the two equations become:

$$\nabla \cdot (\rho \vec{v}) = 0 \tag{3.4}$$

$$-\frac{\partial(pu_i)}{\partial x_i} = \frac{\partial}{\partial x_i} \left[(\rho u_i) \left(e + \frac{u^2}{2} + \rho gz \right) \right] dV$$
 (3.5)

by combining the two equations, the first member of Equation 3.5 is zero, as stated by Equation 3.4 and can be rewritten as:

$$(\rho u_i) \frac{\partial}{\partial x_i} \left[\left(\frac{u^2}{2} + gz \right) + \frac{p}{\rho} \right] = 0 \tag{3.6}$$

The final form of the equation is obtained by differentiating all the terms:

$$\frac{\partial u^2}{2} + gdz + \frac{dp}{\rho} + pd\left(\frac{1}{\rho}\right) = 0 \tag{3.7}$$

Considering the fluid itself, it is possible to assume that the air flowing through the Venturi tube is isentropic, this allow to use isentropic relations of pressure, volume and temperature. Here follows the expression useful for this case:

$$\frac{p}{\rho^{\gamma}} = cost = C \tag{3.8}$$

where ρ is the inverse of the volume, inserting it into Equation 3.7 and considering that its last term is neglected in an isentropic process, to result the following:

$$\frac{\partial u^2}{2} + gdz + C\rho^{\gamma - 1}\gamma dp = 0 \tag{3.9}$$

Then, by performing an integration of Equation 3.9 between two general points in the Venturi and substituting the isentropic relation between density and pressure, the result is:

$$\frac{U_2^2 - U_1^2}{2} + g(z_2 - z_1) + K\left(\frac{\gamma}{\gamma - 1}\right) \left(\frac{p_2}{\rho_2} - \frac{p_1}{\rho_1}\right) = 0$$
 (3.10)

The formulation reached above allows to get to the objective of the project, since the scope is to measure volumetric flow rate, the parameter we need to obtain is the speed of the air in a certain point of the Venturi, ideally the points could be either in the throat or at the inlet, where the diameter is known to a certain value and it is possible to calculate the volumetric flow rate. To derive the formulation for the speed, it is possible to use the continuity Equation 3.4 and obtain a simplified expression for the Equation 3.10. By integrating all over the control volume and assuming a one-dimensional flow, the equation can be written as:

$$\int_{V} \frac{\partial(\rho u_i)}{\partial x_i} dV = \int d(\rho U A) = \rho_2 U_2 A_2 - \rho_1 U_1 A_1 = 0$$
(3.11)

From this formula, the value of U_2 can be derived:

$$U_1 = \frac{\rho_2 U_2 A_2}{\rho_1 A_1} \tag{3.12}$$

inserting equation 3.12 into 3.10 and then deriving the value of U_2 :

$$U_{2} = \left[\left(\frac{1}{1 - \left(\frac{\rho_{2} A_{2}}{\rho_{1} A_{1}} \right)^{2}} \right) \left(\frac{2\gamma}{\gamma - 1} \right) \left(\frac{p_{1}}{\rho_{1}} - \frac{p_{2}}{\rho_{2}} \right) - 2g(z_{2} - z_{1}) \right]^{0.5}$$
(3.13)

Then, the average height of the fluid can be assumed constant during the flow $(z_1 = z_2)$ and substituting the isentropic relation 3.8 in the density value $(\rho_2 = \rho_1 \left(\frac{p_2}{p_1}\right)^{\frac{1}{\gamma}})$ to result:

$$U_{2} = \left[\left(\frac{1}{1 - \left(\frac{p_{2}}{p_{1}} \right)^{\frac{1}{\gamma}} \left(\frac{A_{2}}{A_{1}} \right)^{2}} \right) \left(\frac{2\gamma}{\gamma - 1} \right) \left(\frac{p_{1}}{\rho_{1}} - \frac{p_{2}}{\rho_{1} \left(\frac{p_{2}}{p_{1}} \right)^{\frac{1}{\gamma}}} \right) \right]^{0.5}$$
(3.14)

This formulation is really useful, because allows to apply it in both conditions of compressible and incompressible flow, further manipulation of Equation 3.14 makes visible the coefficient that discriminates from those two types of flow. It is also

possible to derive the simple formulation for only incompressible flow:

$$U_2 = \left(\frac{2\Delta p}{\rho(1-\beta^4)}\right)^{0.5} \tag{3.15}$$

in which the air density is considered constant, β^2 is the ratio between the throat area A_2 and the inlet area A_1 , while Δp is the measured value by the sensor. In our case, it is sufficient to consider an incompressible flow to obtain a reasonable result for the volumetric flow rate. [13]

3.2 Venturi design

The Venturi tube design has been developed following both ISO 5167-4 2003 [14] and ASME PTC 19.5-2004 [15], which give some guidelines to follow about the dimensions of the inlet section and the throat section, as well as the angles for the converging section and the diffuser. The requirements for the design are mainly related to manufacturing constraints, due to the fixed dimension of the 3D printer a Ultimaker S5, which has a chamber volume available for the print of dimension 300x240x300mm, thus the reachable height with the print is limited to the height of the printer. Another constraint for the dimensions comes with the scope of the project, since the Venturi has to be employed within a test bench on the production line the length has to be as low as possible in order to optimize the space and enhance for a compact design.

The prescribed values for the angles mentioned before are $21\pm1^{\circ}$ for the converging section, while for the diffuser the limit is set within an interval between 7° and 14°, in order to avoid fluid separation from the wall and pressure loss at the outlet. The length of the converging part is limited by the diameters at the inlet cylindrical part and of the throat, besides, the diverging section can reach the desired length until

the inlet diameter is reached (Figure 3.1).

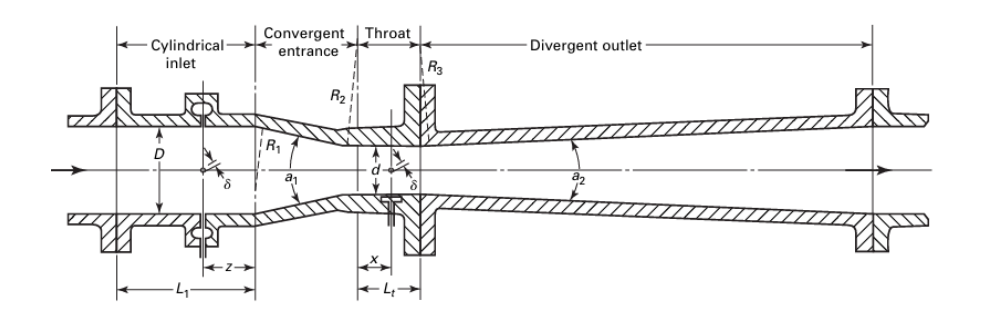


Fig. 3.1: Profile of a Venturi tube. It shows a generic configuration in which all the dimensions mentioned before are indicated. [14]

In Figure 3.1 can be noticed the length of the diverging part being almost half of the whole system, which is the reason for choosing a "truncated" Venturi, the diffuser has a shorter length without reaching the entrance diameter at the outlet. Figure 3.2 shows the outer profile of the Venturi tube used in the project, design choices focused mainly on robustness and ease of handling. The presence of side plates are meant to allow installation on a bench or on a moving device is also visible. On the front face of the tube are designed four holes, available for coupling with the fan to test in a free environment. In the figure the pressure tappings are shown, they are placed in correspondence of the bigger diameter and throat diameter, at distances that follow the normative ([14], [15]).

The inlet diameter D is chosen of 48mm which correspond to the fan opening in order to convey the air flux generated by the fan, while the throat diameter must fall

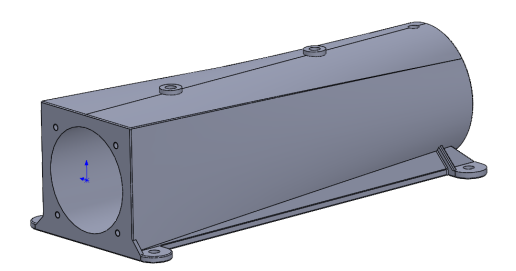


Fig. 3.2: Outer profile of the designed Venturi tube for the project

between 0.25D-0.75D as stated by the ISO standard, in this case throat diameter is 30mm. Following the normative, the converging and diverging angle are of 21° and 14° , moreover the diffuser does not reach the inlet diameter value and thus is considered "truncated", the overall length is of 200mm.

Figure 3.3 also shows the dimension of pressure tappings that are designed to fit with the sensor openings, detail B has to be pointed out as it is meant to hold and secure the positioning of a temperature sensor, it can also be seen from the front view on the left, furthermore, fillet radiuses are designed in proximity of section variation to avoid significant concentrated pressure loss and maintain a constant total pressure head during the flow. By giving a look at the end of the Venturi can be seen a cylindrical canal, whose purpose is to allow the passage of cables for the last mentioned sensor, useful for voltage supply and data exchange.

Some design choices were influenced by 3D printing to obtain a smoother and more efficient process, which will be further explained in detail in the next section.

3.3 Additive manufacturing and CFD simulation

3.3.1 Manufacturing process

The Venturi tube has been fabricated through Additive Manufacturing process, as stated in the introduction AM and 3D printing will be used interchangeably. The 3D printer used is an UltiMaker S5 and employs Fused Deposition Modeling (FDM) technology, it works by adding layers of material to create the object from a 3D model, uploaded previously on the printer software. During the process, each new layer fuses with the previous one by thermal bonding, FDM is the most widely used technology thanks to its low cost, capability and adaptability to a wide range of materials; this technology commonly uses thermoplastic filament, which is heated

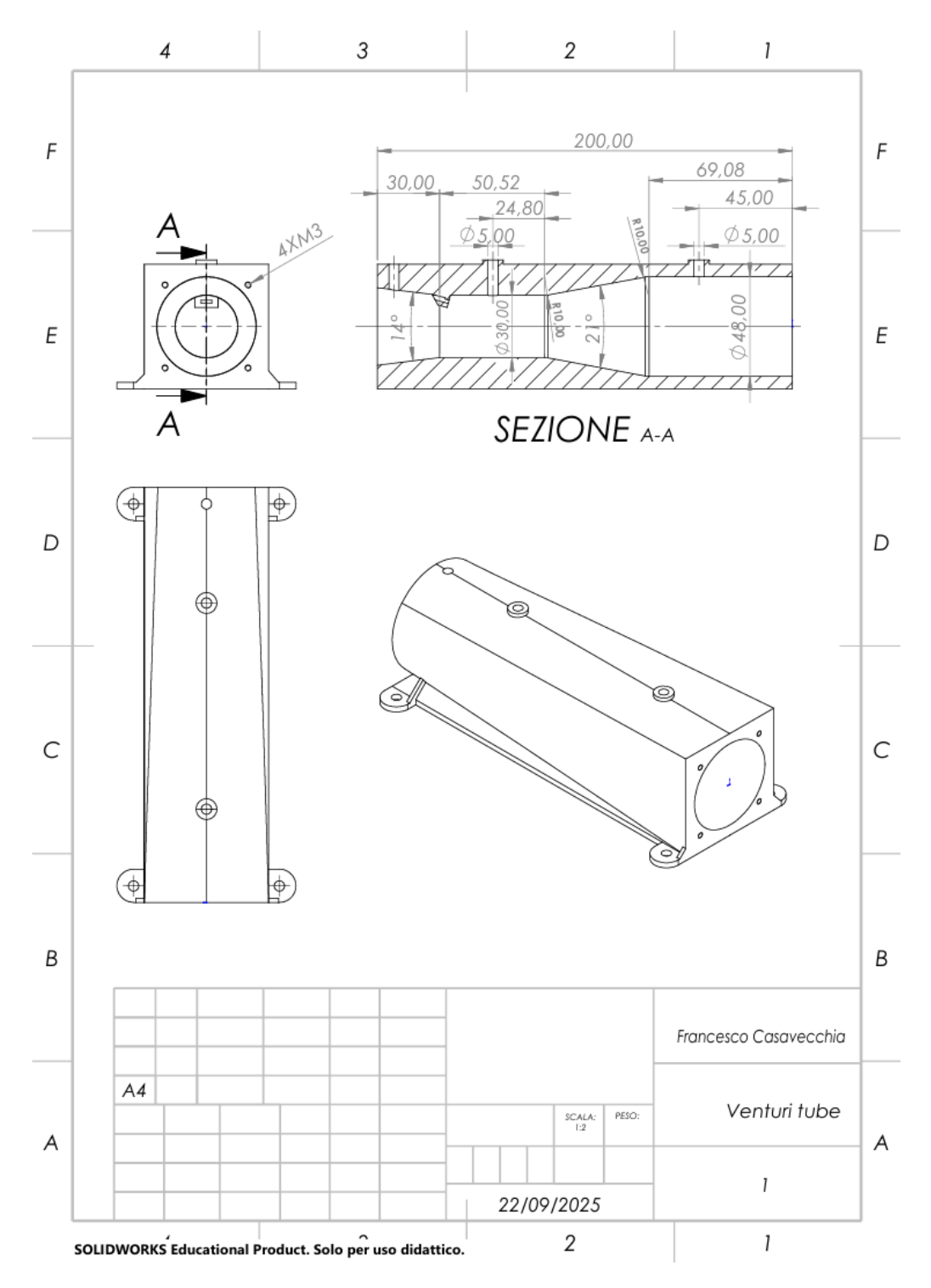


Fig. 3.3: Technical drawing for 3D printed Venturi tube. Section A-A shows the shape chosen for the Venturi with all the fundamental dimensions, also the pressure tappings location are visible. The front and upper view of the Venturi are presented in the drawing. Detail B shows a specific housing for a temperature and humidity sensor.

to a semi-molten state and extruded through a nozzle on the printer platform. This printer also provides different options for the nozzle size, from 0.25mm to 0.8mm, by choosing a larger one the fabrication process can be shortened at the expense of surface quality and precision. For this project a 0.6mm nozzle is used to reduce fabrication time, as a first prototype is acceptable to save time instead of focusing on the best surface finishing. Moreover, the deposition layer is 0.2mm high, which allows to also insert some specific details to the design such as Detail B in the technical drawing 3.3. Overall fabrication time takes about 18 hours, since the printer can run at night, production time is saved.

The material chosen for the tube is PLA, or polylactic acid, defined as a biodegradable thermoplastic polymer derived from renewable resources like corn starch or sugarcane, known for its eco-compatibility and various mechanical properties and it is widely employed in 3D printing applications. In general, steel or other hardened metals are used in the design of Venturi tubes; however, for the low velocity conditions of this project, pressures are expected to be far below the stress limits of the material.



Fig. 3.4: 3D printed Venturi, first prototype. here is shown the Venturi tube from the front part where is visible the inlet but also the thread available to test the fan in a free environment.

Some design choices were influenced by the additive manufacturing process, together with the 3D printing coordinator in the company, we decided to print the Venturi starting from the outlet part and following the axial direction of the tube (image) to optimize material and time usage. It is really useful to avoid using supports in the fabrication, as they are both a material waste and time-consuming, they also do not ensure a precise finishing on the surface supported, for this reason all surfaces have an inclination equal to or higher than 45° with respect to the base platform, this allows us to avoid using supports. The chosen fabrication direction ensures improved definition of circular features, which is particularly important given that the cylindrical inner surface of the Venturi is the most critical geometry.

Additive manufacturing always has advantages and drawbacks, with respect to classical machining technology, AM allows to avoid material waste but employs more time to produce the same object and gives a less precise finish to the surfaces when using simple desktop 3D printer. By the way, in this case, 3D printing is the best option, since it is available directly in the company, without the need to ask an external company for the realization of the Venturi.

3.3.2 Air Flow simulation

Before starting with the experimental procedure, a CFD (Computational Fluid Dynamic) analysis is carried out to virtually test the functionality of the designed Venturi tube. For the analysis, Ansys Fluent software was used together with Ansys Discovery, a new environment available in Ansys that employs the GPU to solve the problem. The 3D model of the Venturi was imported into the software and the fluid volume was extracted from the inside of the tube and simulated, Ansys Discovery was useful to simulate the air flow generated by the fan, allowing to import directly the fan curve shown in figure 2.7 thanks to a more intuitive user interface. The

simulation is conducted in the configuration the fan is operating at its maximum speed (5500 rpm), since it is only possible to upload one curve at a time. For the simulation a shear stress transport (SST) k- ω turbulence model is used, it blends the accuracy of the k- ω model near walls with the robustness of the k- ϵ model in the free stream, making it more accurate and reliable for a wider class of flows [16]. In the simulation, the fluid laying in the pressure ducts is also considered, which allowed me to calculate the static pressure difference between them, obtaining a first measure for the desired parameter and the flow rate. Figure 3.5 shows the simulation results, in particular static pressure contours are displayed with the scale on the side, in addition, the graph in the middle gives the results for differential pressure calculation in correspondence of the two ducts which is around 24Pa.

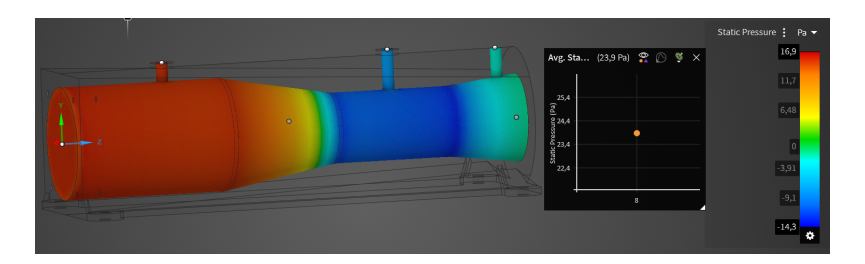


Fig. 3.5: Static pressure contour. On the left the simulated flow in the Venturi, in the middle the differential pressure measurement between pressure tappings and on the right the color reference for static pressure values.

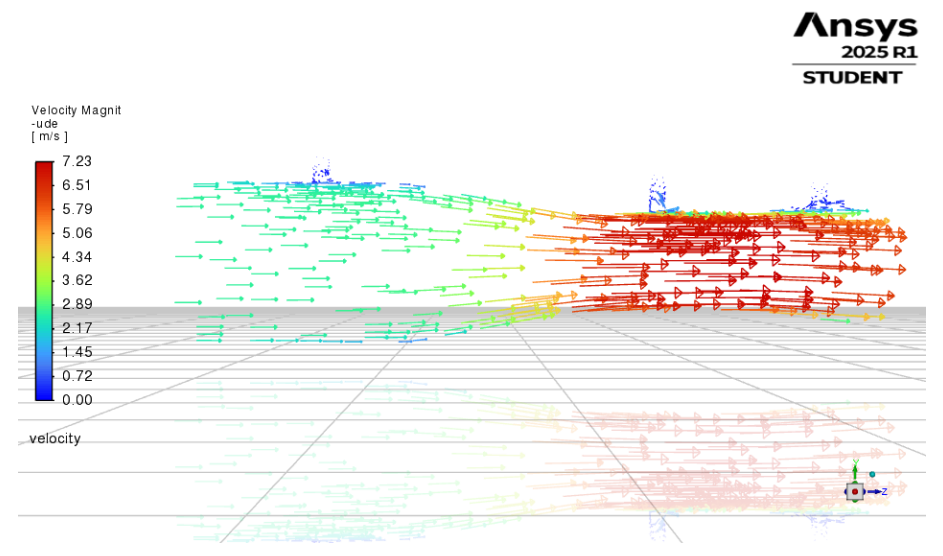
For mesh refinement are used the settings of Ansys discovery having already verified a similar result using a finer mesh near the wall and in correspondence of the pressure ducts. Thus, without overly refining the mesh, a normal computational load is required on the laptop, lowering the number of iterations to reach convergence in the results. The energy model was also introduced into the simulation at first, but did not give any relevant result for the temperature evolution in the Venturi, therefore, this simulation is not taken into account.

A steady-state solver was adopted in order to capture the average performance of the system, since temporal fluctuations and time-dependent evolution are considered to be of minor relevance for the scope of this analysis. Furthermore, a pressure-based solver was selected because the flow can be considered incompressible and occurs at low Mach numbers, where density variations are negligible. This solver is well-suited for internal flows such as ducts or Venturi tubes, providing stable and efficient convergence. Its iterative coupling of pressure and velocity fields ensures accurate prediction of pressure drops and velocity distributions in subsonic conditions.

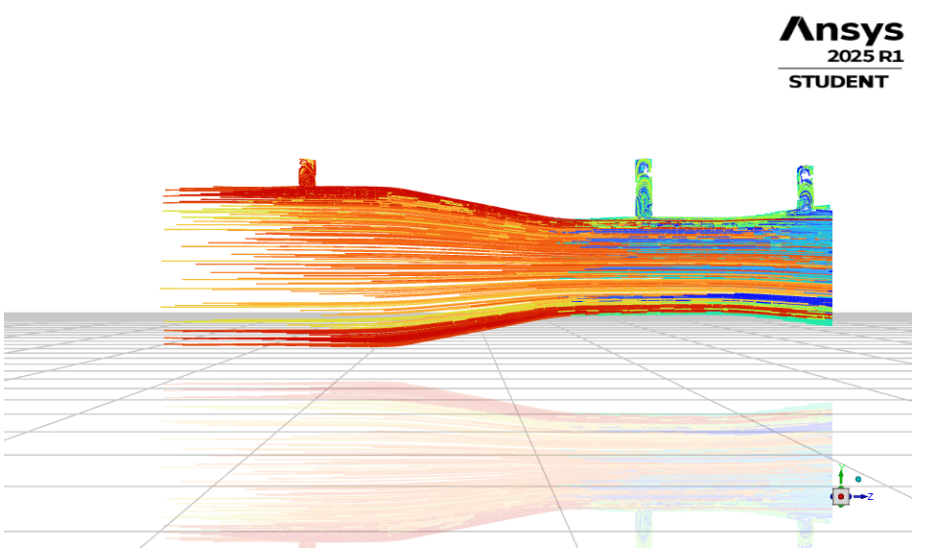
Considered the availability of the fan curve inside the software, the inlet condition type is chosen as intake fan which allows to use the curve and simulate the operation of the fan in this specific system. In correspondence of pressure tappings, velocity equal to zero is chosen as a boundary condition, since the fluid in the duct is stagnating, this condition can be seen in figure 3.6, in (a) is visible due to the small dimensions of velocity vectors (blue in the figure), in (b) where stream lines are represented, are visible some turbulence inside the ducts. The outlet boundary condition is set at constant ambient pressure, because the air flow is discharged in the environment.

In figure 3.6a the velocity regime is shown, it can be observed that, when the fluid passes through the throat section of the Venturi tube, the absolute velocity magnitude undergoes a significant increase, reaching values of up to 7 m/s. This acceleration occurs as a direct consequence of the geometric contraction of the flow section, which forces the streamlines to converge and the fluid particles to move faster in order to conserve mass flow according to the continuity principle (3.2). Despite this rapid acceleration, the velocity vectors remain predominantly aligned with the main flow direction, indicating that the flow maintains its axial character without introducing significant deviations or recirculation in this region.

The velocity ranges between 3 and 7 m/s, therefore compressibility of the fluid is negligible due to the compressibility factor value ϵ close to 1.



(a) Velocity vectors inside Venturi tube. Shows the trend of velocity inside the tube, visible is its variation when going through the throat section, causing an acceleration of the flow.



(b) Air flow stream lines. Shows the path followed by the fluid particles both inside the ducts and the Venturi itself.

Fig. 3.6: Evolution of the flow inside the Venturi. Velocity trend and stream lines.

Chapter 4

Sensors and electronics set up

In the project, sensor technology plays a major role in obtaining a complete characterization of internal flow, therefore, an accurate analysis and selection has been performed, in order to ensure the most precise measurement. The process is supported by an Arduino Zero board that allows to interconnect all the devices and acquire data.

4.1 Sensors selection

The main objective of characterizing air flow is achieved by analyzing and choosing the best sensing solution, which ensures reliability and precision. As stated in the previous chapters, the intended variables to measure are the differential pressure between the inlet section and the throat section, as well as the humidity and temperature of the airflow, pointing out that the differential pressure value will be directly used to measure volumetric air flow through equation 3.15. An SDP810-500Pa is chosen as differential pressure sensor, while an SHT85 sensor is selected for humidity and temperature measurement, both the sensors are manufactured by Sensirion. Both the sensors employed in this system are of the digital type, a feature

of considerable relevance from a signal processing perspective. By providing a direct digital output, these sensors enable immediate integration with digital processing units, thereby eliminating the necessity of an intermediate analog-to-digital conversion stage. This not only streamlines the system architecture but also enhances overall reliability by reducing conversion-induced errors, lowering susceptibility to noise, and improving both processing efficiency and temporal resolution. In addition, for the sensors the Arduino libraries are available directly online, this speeds up the process of data acquisition and processing, without the need to create the functions specific for each sensor from the digital signal.

4.1.1 SDP810-500Pa

The differential pressure is measured by a thermal sensor element using flow-through technology, it detects a pressure difference via temperature measurements of a continuous gas stream through the sensor, this technology allows for highest sensitivity at low differential pressures and have no zero-point drift, in contrast with other type of sensors like membrane ones in which at low pressure difference (low flow rates) the sensitivity decreases. The absence of any moving parts inside, leads to zero-point offset stability and long lifetime, and eliminates the need for recalibration or any maintenance action. The sensor has a measurement range from -500Pa to 500Pa with an accuracy of 0.1Pa and can give an output signal with a maximum response time of 3ms, it can perform measurement within a temperature range between -40 to $+85^{\circ}$ C. From an electrical point of view, the sensor is powered by a 3.3V pin of Arduino Zero, but can support up to 5V voltage supply, signal communication is realized through I^{2} C Protocol with the microprocessor.

Differential pressure measurement can be made in multiple ways, either with continuous measurement and the sensor always providing an output or in a trigger-based measurement mode in which the microprocessor explicitly requests the sensor output at a specific instant in time, the sensor is in idle state by default in this configuration and wakes up only when the command is sent. [17]



Fig. 4.1: Differential pressure sensor SDP810-500Pa. [17]

4.1.2 SHT85

The SHT85 is an high-precision sensor developed to measure relative humidity (RH) and temperature by means of advanced technologies. Relative humidity measurement is performed by a capacitive type sensor which consists of a hygroscopic dielectric material placed between a pair of electrodes that forms a small capacitor. The measured capacitance of the device changes as the dielectric material absorbs or loses moisture in proportion to the relative humidity of the surrounding air. On the other side, the temperature is measured through an integrated band-gap semiconductor sensor, this class of sensor relies upon the temperature-dependent voltage characteristic of a silicon diode.

In terms of humidity measurement, the accuracy tolerance is around $\pm 1.5\%$ with



Fig. 4.2: Humidity and temperature sensor SHT85. [18]

high repeatability up to 0.08% and a response time of 8s covering the full range of humidity percentage (0-100%), while when measuring the temperature, the sensor reaches an accuracy tolerance of ± 0.1 °C, combined with a high repeatability up to 0.04°C. The sensor shows best performance when operating between 5-60°C and 20-80%RH, and any calibration action is automatically performed.

For electrical specification, it must be underlined that the sensor is supplied with 3.3V voltage (5V voltage supply available), and similarly to the SDP810 the communication with Arduino board is performed through I²C protocol. This sensor is designed to operate in two distinct measurement modes, thereby offering flexibility depending on the requirements of the application. The first option is the single-shot mode, in which the device performs a single measurement only when requested, making it particularly suitable for applications where power consumption must be minimized. The second option is the continuous acquisition mode, in which the sensor repeatedly collects data over time, providing a steady stream of measurements that can be directly integrated into real-time monitoring or control systems to automate the data acquisition process.

This type of sensor has been selected in favor of a simple thermocouple which usually has smaller resolution and accuracy. [18]

4.2 Digital part and system connection

This section will provide an overview about I²C communication and its working principle, then will be presented the digital part developed for the project through the Arduino Board and how sensors and all other devices have been integrated, showing also directly on the oscilloscope the I²C communication between the devices.

4.2.1 I^2C Protocol

The Inter-Integrated Circuit (I²C) bus is a widely used serial communication protocol originally developed by Philips Semiconductors and standardized in its official specification. It is based on a two-wire interface, consisting of a serial data line (SDA) and a serial clock line (SCL), which enables multi-master and multi-slave communication (Figure 4.3) with minimal wiring.

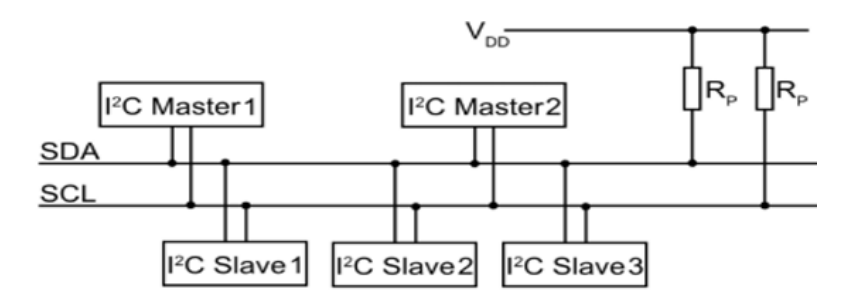


Fig. 4.3: I2C Multi-master Multi-slave Configuration. [19]

The two wires carry information between the devices connected to the bus, each device is recognized by a unique address and can either transmit or receive information depending on its function. Data transfers are synchronous and organized in 8-bit frames, each acknowledged by the receiver to ensure reliable communication. The bus supports a range of speeds, from Standard-mode (100 kbit/s) and Fast-mode (400 kbit/s) to High-speed mode (3.4 Mbit/s), offering flexibility depending on system requirements. Control of the bus is managed by a master device (gener-

ally a microcontroller), which generates the clock, initiates transactions, and issues START and STOP conditions to delimit communication. In Figure 4.3 are also visible two resistors respectively connected to SDA and SCL wires and to the supply voltage of the system (usually 3.3V or 5V), their purpose is to maintain HIGH the logic level when the system is in idle state, but when the communication starts, the microcontroller takes the "control" of the line and transmits the data by using the resistors to maintain HIGH the signal and internal "switches" called mosfets to put down the signal at logic level LOW.

When the bus is free, both SDA and SCL signals are HIGH (or "1", here the level of the logic is intended), the communication starts when the master changes SDA from HIGH to LOW and clock stays high, this is called START condition. The first byte transferred includes the slave address (7 bit) and the read or write instruction (R/W, 1 bit) which informs whether the master wants to read from the slave or write to the slave, the Read (R) instruction corresponds to 1 while Write (W) is 0. Every byte transmission is followed by an acknowledge bit (ACK) which ensures that the addressed device is available for receiving or delivering data, after there are one or more bytes that transmit the data information either from the slave or the master and each of them is followed again by an ACK bit from the data receiver. When all the data information are exchanged by the two devices, the master interrupts the communication by transition of SDA from LOW to HIGH while SCL is HIGH, this is called STOP condition. All the process described above is directly visible in Figure 4.4.

In addition, arbitration and clock synchronization mechanisms allow multiple master devices to coexist without data corruption, while features such as clock stretching enable slower slaves to delay the master when additional processing time is needed. These characteristics, combined with its low pin count and simplicity, have made I²C a standard for communication between microcontrollers, sensors, memories, and

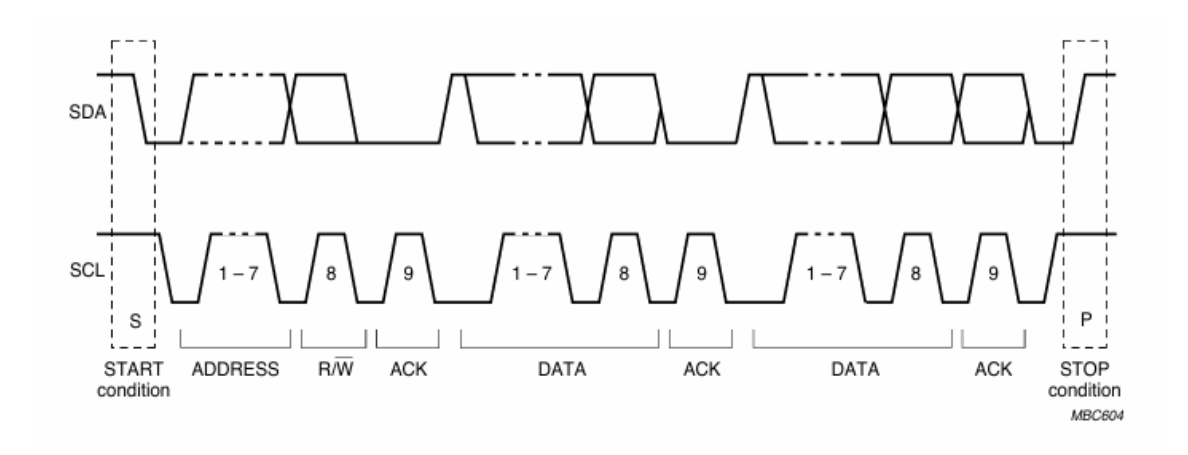


Fig. 4.4: Data transfer on the I2C-bus. [20]

other peripherals in embedded and consumer electronic systems. [19] [20]

4.2.2 Digital system connections

Most of the system is managed by the Arduino Zero board, which has the role of communicating with both the sensors through I²C protocol and process the data read from the differential pressure sensor and the humidity and temperature sensor.

In Figure 4.5 is shown how the connections have been managed, in particular, a small breadboard is used to canalize the SDA and SCL lines from the sensors to the single port of the Arduino board. The same strategy is used to power the sensor with the 3.3V voltage supply and connect them to the GND port. The sensors present a different inter-pin distance which require the use of two distinct types of connectors for proper integration. From the figure above is visible the location where the SDP810 sensor connects with the Venturi tube.

In the real set up the connection is performed by using rubber pipes which have the same diameter as the sensor ports and specific connectors are employed to connect the pipes to the Venturi taps, since it is the first prototype to be analyzed, the pipes are not permanently sealed to the Venturi nor to the differential pressure sensor in

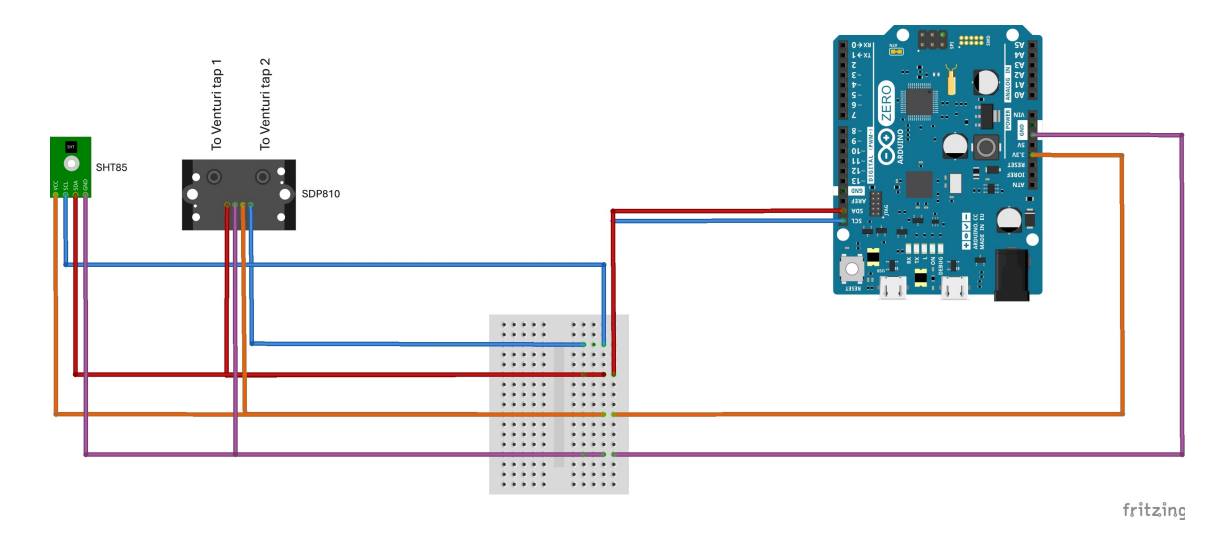


Fig. 4.5: Sketch of wiring between Arduino and the SDP810, SHT85. Shows the arrangement of the system and how the cables are interconnected to reach the Arduino, starting from SDA (red) and SCL (blue) and then power supply (orange) and GND (purple).

order to operate freely any changes to the system and reuse the sensors without damaging it. The SHT85 sensor is mounted inside its dedicated location within the tube and is visible in Figure 4.6 through the white cables.

4.2.3 Sensors identification

Before starting the measurements and acquisitions, an I²C device scan is performed through Arduino board, an *ad hoc* script is used to directly obtain the addresses in hexadecimal number corresponding to all I²C devices connected to the board. From the sensors datasheet is possible to extract the address both is hexadecimal and binary, the SDP810 address is 0x25 (b. 0100101) [17] while the SHT85 address is 0x44 (b. 1000100) [18], here is verified what has been previously mentioned in section 4.2.1 about the 7 bit length of the I²C devices address.

From the serial monitor in Arduino software three devices have been identified corresponding to three addresses: 0x25, 0x44, 0x28; the first two identify respectively the differential pressure sensor and the humidity and temperature sensor, the third one

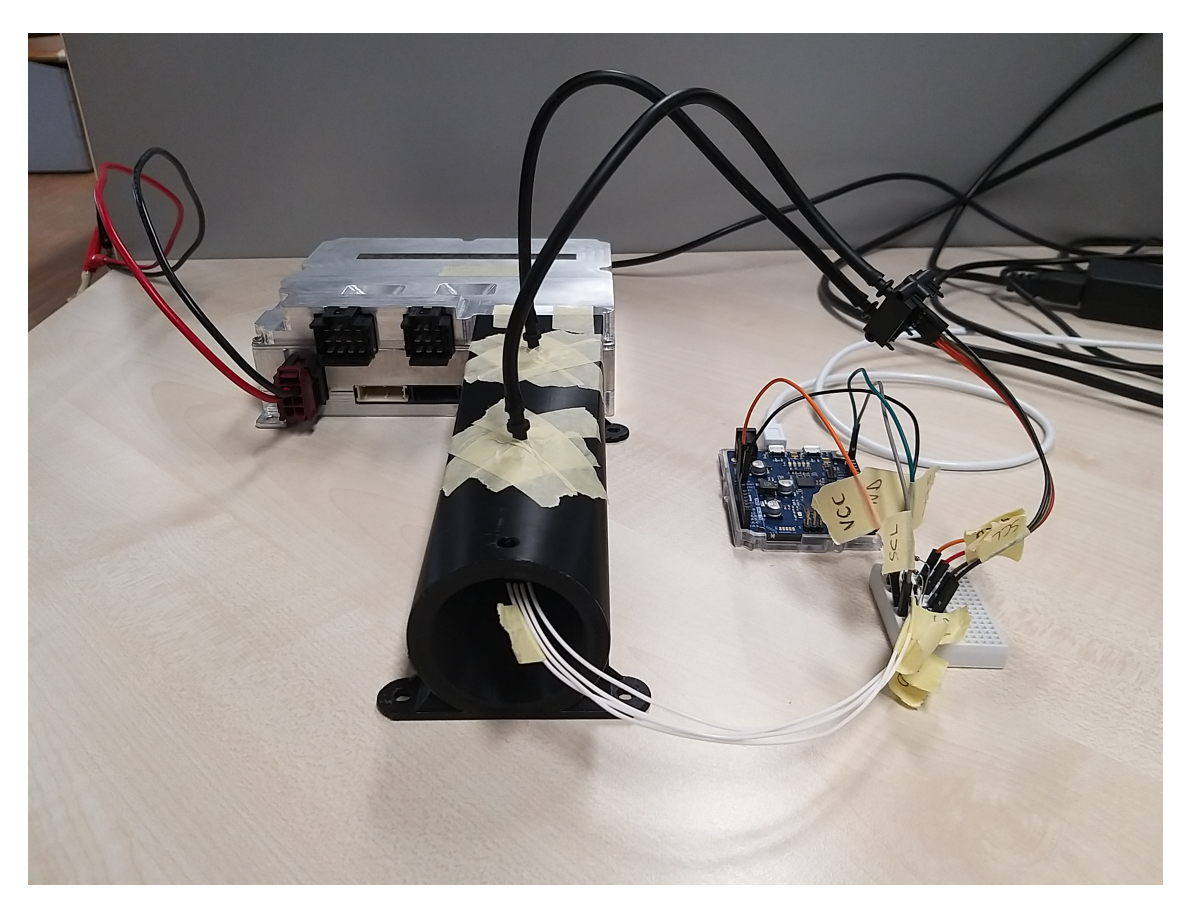


Fig. 4.6: Experimental set up for air flow measurement. Shows in the background the ECU used for the project, the 3D printed Venturi tube and all the electronics use for the data acquisition comprehensive of the sensors, a breadboard and the Arduino Zero board.

is probably referred to a device inside Arduino board. This match ensures that the sensors are correctly connected to the board and measurements can be performed. In Figure 4.7 is represented an analysis conducted with an oscilloscope in which is captured the I²C communication between the Arduino and the sensors. In the acquisition are visible three bursts of communication, the red band identifies the address of the device and the rest of the acquisition contains the instructions delivered by the microcontroller. Considering the first burst as an example, the red band reads hex. 4b (b 01001011) in the first byte, from section 4.2.1 we know that only the first 7 bit identify the address while the last bit refers to the read or write instruction, thus in this case the address is b 0100101 (hex 25) and corresponds to

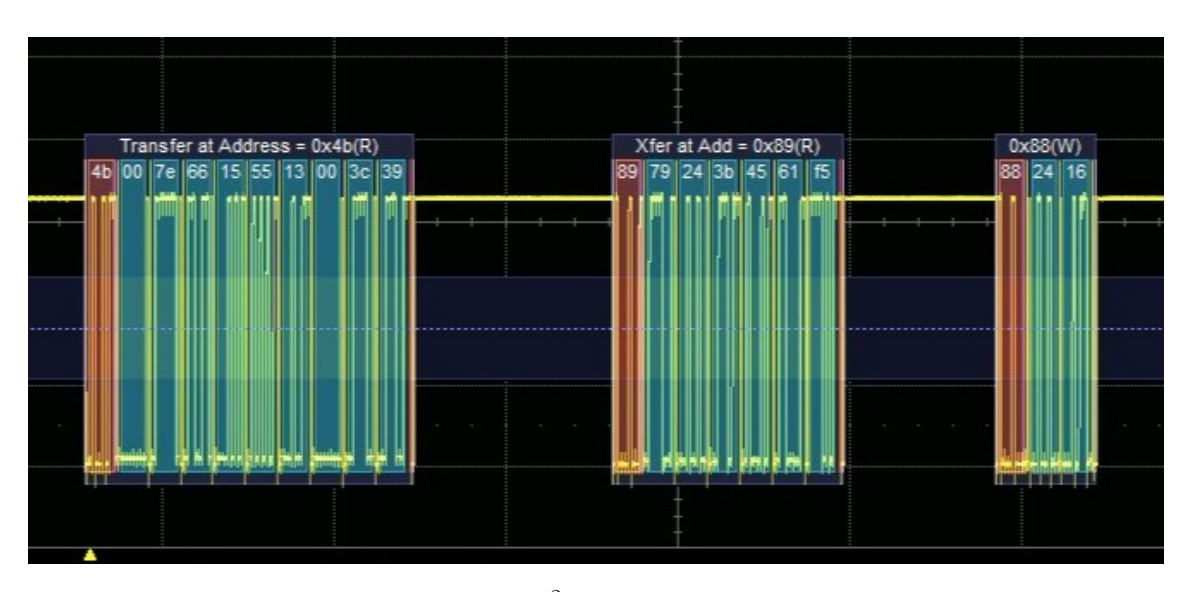


Fig. 4.7: Oscilloscope acquisition of the I²C communication between Arduino Zero board and the sensors. Shows the data bursts in which the information is stored, verified the theoretical review of section 4.2.1 about the I²C communication protocol.

the SDP810 sensor which is requested to be read by the master.

For the other two bursts, the first bytes are 0x89 (b 10001001) and 0x88 (b 10001000), in this case the 7 bit address is 0x44 and is the same for both data acquisitions, so refers to the same device (SHT85), only changes the R/W instruction from the microcontroller, the following bytes carry information about the instruction the sensor has to follow, for example, the measurement command or the read information from the sensor.

4.3 Arduino Script

The acquisition process with the Arduino board comes with the necessity to develop an Arduino script which is used as an interface with the microcontroller. The Arduino IDE allows to write the program, upload it directly into Arduino board and execute it. The script is available for consultation in Appendix A and is used only to control the sensors, as mentioned above. The code allows the communica-

tion by initializing the serial port and the I²C protocol, the baud rate is chosen of 115200 bps meant for future integration with the fan control managed directly by the ECU which communicates at the same rate. The specific communication with the sensors is set through their own libraries available directly on the Arduino IDE, those libraries allow to perform any type of instruction possible (the same listed in the datasheet, [17] [18]) for the sensors and it is possible to review them through the corresponding header file (.h).

The Arduino code fully automates the process of acquisition from the sensors, continuously iterating on the given instructions. The Arduino is aided by a Python script which has the simple purpose of acquiring Arduino output and exports the data directly into an Excel file where are available for further data analysis. The loop performed in Appendix A follows a simple cycle, stating with the acquisition from the sensors, it first requests the SDP810 to give the differential pressure and the temperature values which are both available at this sensor through its library function that applies autonomously the scale factors to the measured value, in particular, the differential pressure value is then used to calculate the volumetric flow rate (m^3/min) with the Equation 4.1 [13], after that all the variables are printed on the serial monitor.

$$Q = C \pi \left(\frac{d}{2}\right)^2 \left(\frac{2\Delta p}{\rho \left(1 - \beta^4\right)}\right)^{0.5} \tag{4.1}$$

The same procedure is used for the humidity and temperature sensor (SHT85), to which the values of humidity and temperature through two different functions available in its library are requested and again printed on a new line of the serial monitor. Before the loop restarts, the system waits 5000 ms to allow the SHT85 sensor to perform its calculation and communicate the values.

Chapter 5

Data acquisition and testing solution

The realization of a testing procedure requires a background research that aims to acquire a sufficient amount of data to develop a general characterization of the system that allows to establish a standard working condition and with which is possible to build a fully reliable process that considers an acceptability range for fan testing.

5.1 Acquisition process

As mentioned in chapter 4, the acquisition system is composed of an Arduino board on which a specific code developed directly on the Arduino IDE is uploaded, the acquisition chain includes data processing by a Python code (Appendix B) that reads directly the values from the serial port of the Arduino and repeatedly exports all the data into an Excel file. Moreover, the code autonomously detects when the fan speed changes by evaluating the value of differential pressure read by the sensor, if the difference with the previous value is over a certain threshold, it asks the user

to insert the changed Duty Cycle value which corresponds to a certain speed value, then is inserted in the first column of the output file. Thus each row of the data reading contains the DC, differential pressure, volumetric flow rate, humidity and temperature values.

Before starting the acquisition in the laboratory, all cable connections are checked to avoid any damage to sensors and other devices, after that, all the set-up is powered on and correct working of the fan is verified. From the HMI (Human Machine Interface) of the ECU the process is started by applying first a 30% DC to the fan DC motor, this value is the minimum to start the motor by overcoming the inertia and the motor electrical losses. Consequently, the procedure continues by increasing the duty cycle by 10% after obtaining at least five acceptable value readings, taken after a transition time in which the fan reaches the desired speed and the air flux completely develops inside the Venturi.

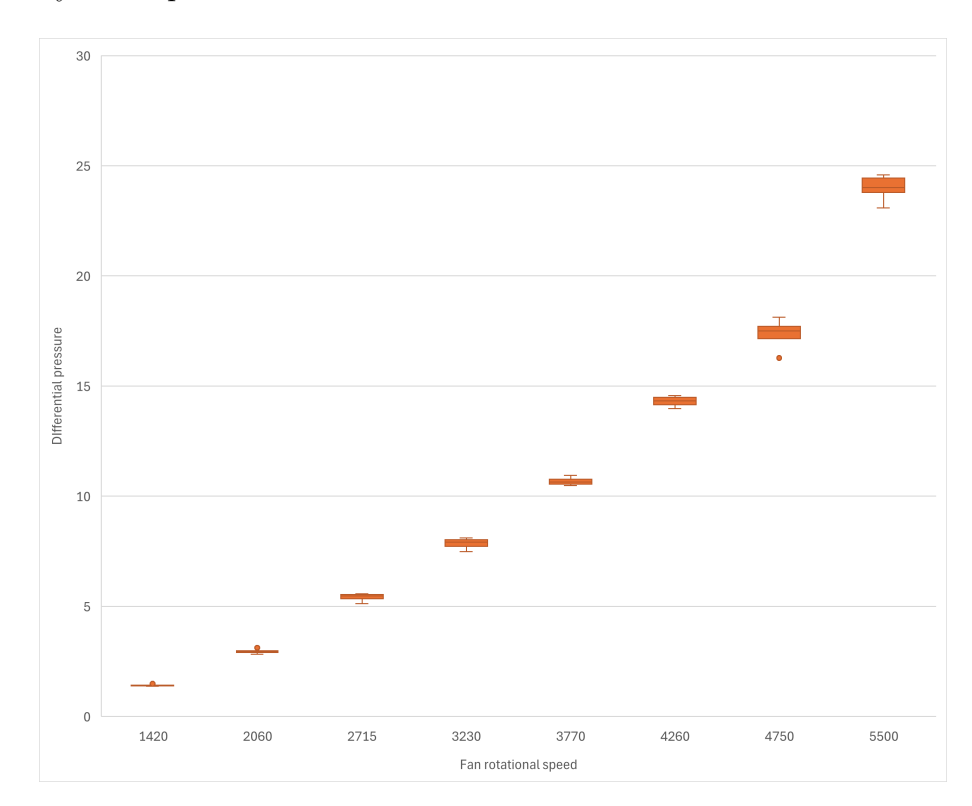


Fig. 5.1: All data acquired plotted in a speed - differential pressure graph.

In Figure 5.1 the acquired data are shown and it is visible at first glance that the more the speed increases, the higher is the variability in the values, in fact the boxes in the graph increase in size with speed increase. The acquisition process continues by selecting only the data obtained at certain DC values, in particular 40%, 60%, 80%, 90% and 100%, the decision was based on the fan performance curves reported in the datasheet, as these curves allow the subsequent characterization of the system.

5.2 System characterization and working point

The process of characterization and data elaboration requires the fan curve to be available in the Excel file through the aid of online tool to extract the curve points, it is then possible to explore with further analysis the overall functioning of the fan and Venturi system. In terms of fan characterization, also an overall efficiency evaluation is carried out, bringing to the light the low total efficiency at which this kind of cooling fans operates. In this case, the efficiency at 100% DC is investigated and in Figure 5.2 is visible the trend at all the operating points of the fan (orange in the picture), it is possible to expect the fan to work in an interval between 0.22 and $0.37 \ m^3/min$ where the efficiency reaches the highest values. The same is expected to happen when the fan operates at lower speeds.

The objective of sensors employment lies directly in characterizing the overall system, given that when, for example, a turbomachine is adopted within a piping system, further analysis is required to understand the mode of operation of the system and to verify whether it constitutes the most appropriate solution for the given application. In particular, the point to investigate is the interaction of the turbomachine, a fan in this case, and the system to which is connected, and this is called working point, or in other words, is the intersection between the fan performance curve and the system resistance curve, which in this case are both available.

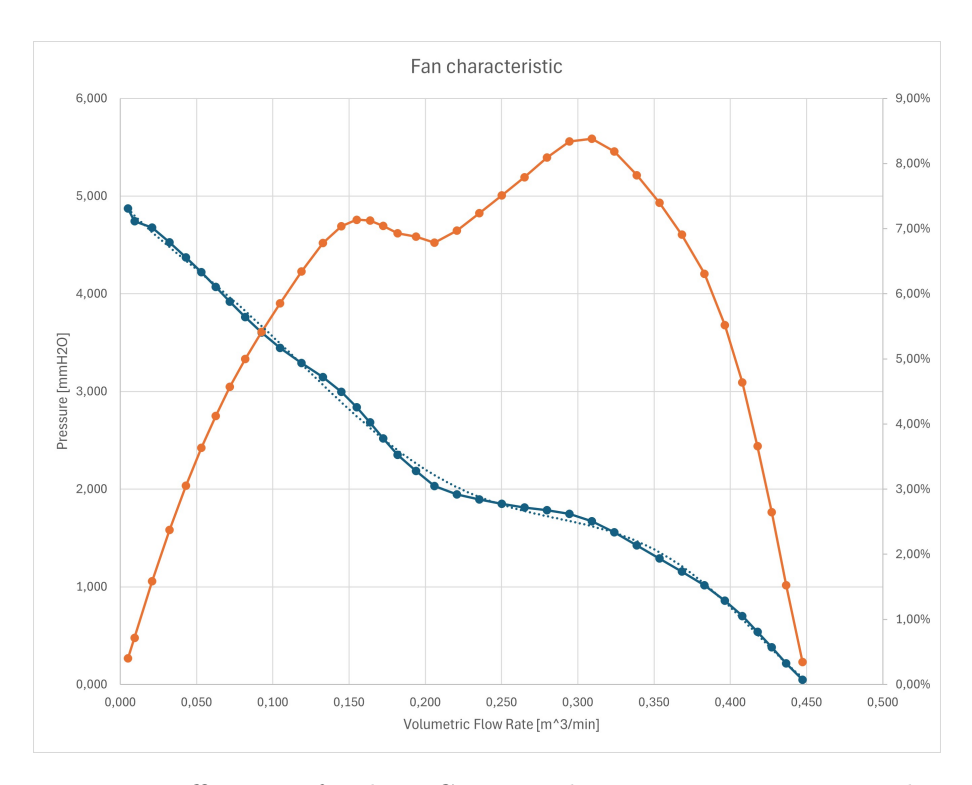


Fig. 5.2: Efficiency of Delta DC Fan working at its maximum speed.

From Figure 5.2 is reproduced the fan performance curve (blue in the picture), while to obtain the system resistance curve it is necessary to refer to the Darcy-Weisbach equation (Equation 5.1), valid for incompressible flow in steady state condition which describes how the fluid evolve within a pipe, in particular defines the evolution of pressure losses and essentially expresses the quadratic proportionality between Δp and the volumetric flow rate Q.

$$\Delta p = f \frac{L}{D} \frac{\rho v^2}{2} = f \frac{L}{D} \frac{\rho}{2} \left(\frac{Q}{A}\right)^2 = k Q^2 \tag{5.1}$$

It is possible to apply directly in this project the considerations made above and find the working point of the fan where its performance satisfies the demand of the system. The process involved finding all the fan working points for the desired speeds; therefore, for each fan speed the data acquired identify both the differential pressure and the flow rate at which the system is working and through the different fan curves the system resistance curve is identified. The characterization is performed for two cases, the first when the fan is outside the ECU and is free to intake air from the surroundings, the second is the real working condition inside the ECU where intakes the air.

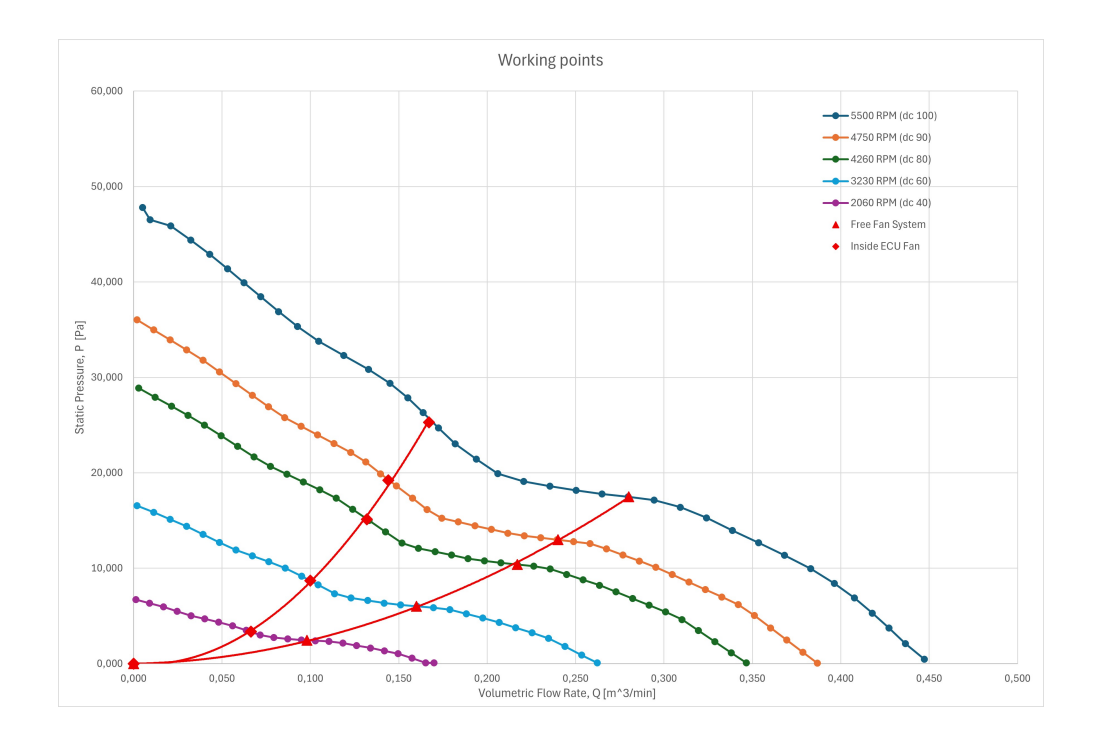


Fig. 5.3: Working points identified for each fan speed.

A first data elaboration leads to the identification of the system resistance curve in both configurations (Figure 5.3), when the fan works inside the ECU the flow encounters more resistance, as expected and the air flow generated by the fan is limited. Anyway it is possible to reach a stable condition to acquire the proper values from the sensors and generate the system curve. With respect to the efficiency, the fan works in the acceptable interval, which is verified to be the best solution for the application. The configuration in which the fan is outside the ECU is taken as a reference, since the performance is not influenced by the obstructed environment

inside it, verifying the hypothesis of a higher flow rate provided by the fan.

5.3 Acceptability range for testing

The process now intends to obtain a standardized method to assess whether a test passes or fails, in this view, the strategy followed is to set an interval of values in which the tested product is meant to fall to pass it. Therefore, the identification of a range comes directly from the values acquired by the digital setup and among a wide amount of data the highest and lowest values can be considered to identify the end points of the interval, this procedure is followed for each of the fan speeds for which is tested the device.

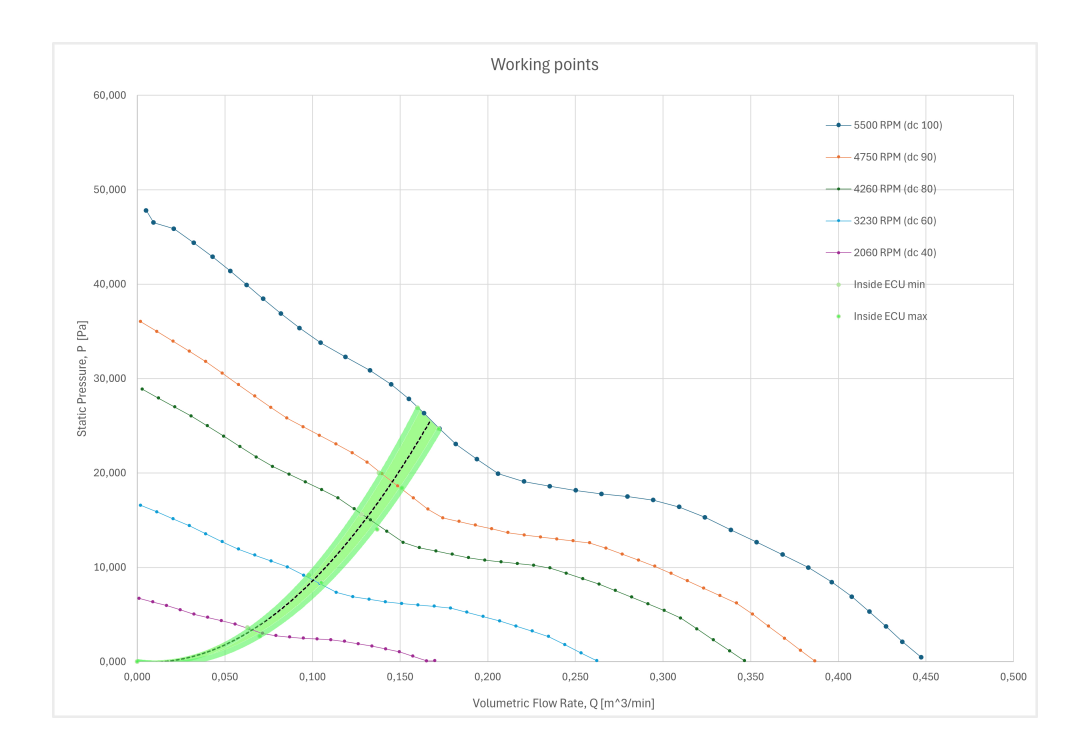


Fig. 5.4: Acceptability range identified on the fan curve. Here is displayed the estimated area in which a DUT has to fall to pass the test

This solution does not exclude that some device could fall in a gray zone, a situation in which even if the test fails and discarded by the operator, it could still be accepted at discretion of a supervisor that evaluates the effective problems with the DUT (Device Under Test), if it works properly and in case of positive judgment, is accepted. In Figure 5.4 the approximate calculated area in which the test is valid is visible on the graph, thus showing the acceptability limits for a fan. But in the real application of the testing process within the production line, the data to be used are summarized in Table 5.1, the system will calculate the value of the volumetric flow rate and will verify whether it falls within a certain interval, the operator will receive the pass or fail signal from the system itself. The system is also meant to provide a signal of possible failure, when the measured value remains within a certain percentage (to be determined) of deviation from the upper and lower range values.

SPEED [rpm]	INTERVAL $[m^3/min]$
2060	0.063 - 0.070
3230	0.098 - 0.105
4260	0.128 - 0.137
4750	0.138 - 0.151
5500	0.160 - 0.172

Tab. 5.1: Acceptability range of Volumetric flow rate related to each speed value.

Conclusion

The main objective of this project was to realize a reliable procedure to study the airflow generated by a fan employed in automotive infotainment systems and determine acceptance criteria for a testing solution. The project outcome ensures the possibility to create a dedicated test bench to be successfully inserted into the production line.

In the project was developed the complete design of a Venturi tube following the specific ISO and ASME standards and was then realized through additive manufacturing process, directly available in the company facilities. It allowed to build the testing process for the fan, using its specific characteristic of section variation to measure the pressure change in the fluid, which then is used to determine the volumetric flow rate generated by the fan. The study of the air flow is carried out satisfactorily, reaching the conclusion of negligibility of fluid compressibility, being able to simplify the analysis for incompressible air flow due to the low speeds involved in the system, ranging from 3 to 7 m/s, results also available through the CFD simulations (Figure 3.6a).

The data were actively acquired using a digital differential pressure sensor connected to an Arduino Zero board, which processed the digital signals to provide usable values for subsequent analysis in Excel. These data were then employed to determine the fan operating points and define the corresponding acceptability ranges required for the testing process. The results showed the possibility of developing a fully

working testing bench to be positioned as End of Line test by applying the findings obtained in chapter 5. The temperature and humidity sensor gave precise and responsive values, but unfortunately it was not possible to produce a substantial procedure that would include them in the testing process, it gave anyway a more complete characterization of the air flux.

This project not only gave a complete analysis to proceed with the development of a test bench, but most importantly set the method to use for future company products. This analysis is carried out referring to the ARTIST10 platform, which presents certain characteristics, but the next platforms could include different cooling fans with which it will be necessary to apply again the acquisition process and obtain new data and new acceptability ranges.

Future developments

Future work will mainly focus on developing a complete test bench which will allow the operator to simply insert the ECU platform and perform the test. This results comprises the development of a dedicated digital acquisition system, in particular a specific PCB to avoid using the Arduino board and to remove all the unnecessary components and interfaces. Ideally, the best solution could directly involve the ECU to control and process all the system data.

Moreover, the surface finishing of the Venturi could be improved by choosing a different manufacturing process that could lead to cleaner results, in addition it will be necessary to repeat the analysis for a smaller fan (dimensions, 40x40x15mm) that could allow to realize a smaller housing of the ECU. In the end, the temperature and humidity readings could be further investigated to be employed as a back-up test or complementary test.

Appendix A

Arduino code

The following appendix reports the full Arduino sketch used in this project.

```
1 /*
2 SENSOR DATA ACQUISITION
_{\mbox{\scriptsize 3}} - Differential pressure sensor
4 - Humidity and Temperature sensor
6 #include <Arduino.h>
7 #include <Wire.h> //include I2C communication library
8 #include <SensirionI2CSdp.h> //sensor library
9 #include <SHT85.h>
10 #include <math.h>
12 #define SHT85_ADDRESS
                                   0x44
13 #define pi 3.1415
_{\rm 15} SHT85 sht85(SHT85_ADDRESS); //definition of temperature and
     humidity sensor
16 SensirionI2CSdp sdp; //definition of differential pressure sensor
18 #include <Pressure.h>
```

```
19 diff_pressure p;
20 char errorMessage[256];
21 float D1 = 0.048; //inlet diameter
22 float D2 = 0.03; //Throat diameter
23 float C = 0.92; //Discharge coefficient
24 float Area = pi*(pow(D2,2))/4; //Throat Area
25 float air_density = 1.23; //[kg/m3]
26 float d = D1/D2; //diameter ratio
28 void setup() {
    // put your setup code here, to run once:.
30
    Serial.begin(115200); //initialization of serial setting 115200
31
     bps, opening serial port
    while (!Serial); //while comunication is open
    Wire.begin(); // Initialize I2C communication
33
34
    sdp.begin(Wire, SDP8XX_I2C_ADDRESS_0); //initialize sensor
     communication with arduino by defining sensor address
    sdp.startContinuousMeasurementWithDiffPressureTCompAndAveraging()
     ; //start of continuous measurement with temperature
     compensation, see datasheet for more details
37
    if (!sht85.begin()) {
    Serial.println("Sensor not found!");
40 }
41
42 }
44 void loop() {
    /*
    -----Differential Pressure Reading-----
```

```
*/
47
    float differentialPressure;
    float temperature;
    uint16_t error = sdp.readMeasurement(differentialPressure,
50
     temperature);
    if (error) {
51
          Serial.print("Error trying to execute readMeasurement(): ")
52
          errorToString(error, errorMessage, 256);
53
          Serial.println(errorMessage);
    } else {
55
          Serial.print(differentialPressure); //dP value
56
          Serial.print(",\t");
          float massflow = 60*C * Area * sqrt(2 * fabs(
     differentialPressure) / (air_density*(1-0.16))); //Volumetric
     flow rate [m<sup>3</sup>/min]
          Serial.print(massflow,3);
59
          Serial.print(",\t");
60
    }
63
64 /*
65 -----Temperature and Humidity Reading -----
    if (sht85.dataReady()) {
67
      sht85.readData();
68
      Serial.print( sht85.getTemperature(), 1);
69
      Serial.print(",\t");
70
      Serial.println(sht85.getHumidity(), 1); //Humidity value [%]
71
      sht85.requestData();
    } else {
73
      Serial.println("data not ready");
```

```
75  }
76  delay(5000);  //wait for next measurement
77 }
```

Listing A.1: Arduino Code employed for data acquisition

Appendix B

Python code

Here is shown the python code employed to export data from Arduino to Excel

```
1 def main():
2
      import serial
3
      import time
      ser = serial.Serial('COM11', 115200) # COM port of Arduino
      time.sleep(2)
      with open("data_log.csv", "w") as file: # create Excel file
7
8
          file.write(f"DC [%];DiffPressure; MassFlow;Temperature;
      Humidity\n")
          dp = 0 # initialize differential pressure variable
9
10
          while True:
11
12
               if ser.in_waiting > 0:
13
14
                   line = ser.readline().decode('utf-8').strip() #
      read from the serial
                   row = line.split(",")
15
16
                   if len(row) == 4:
17
```

```
i = 0
18
19
                        for i in range(4):
20
                            row[i] = float(row[i])
                            i = i + 1
21
                        if abs(dp - row[1]) \le 0.015: # condition for
22
      DC change
23
                            dp = row[1]
24
                            print(f"{row[0]} {row[1]} {row[2]} {row[3]}
      ")
25
                            file.write(f"{dutycycle};{row[0]};{row
      [1]};{row[2]};{row[3]}\n")
                            file.flush()
26
27
                        else:
                            dutycycle = input("DC value: ")
28
29
                            dp = row[1]
                            print(dutycycle)
30
                            print(f"{row[0]} {row[1]} {row[2]} {row[3]}
31
      ")
32 main()
```

Listing B.1: Python script for data analysis and plotting.

Bibliography

- [1] International Organization for Standardization and ASTM International, "ISO/ASTM 52900:2021, Additive manufacturing General principles Fundamentals and vocabulary,", Geneva, Switzerland, 2021.
- [2] International Organization for Standardization, "ISO 4006:1991: Measurement of fluid flow in closed conduits— Vocabulary and symbols", Ed.2, 1991.
- [3] Alan S. Morris, Reza Langari, "Measurement and Instrumentation: Theory and Application, Third Edition", Academic Press, 2021, Pages 499-534
- [4] Universal Flow Monitors, Inc., "Thermal Flow Meter Technology", flowmeters.com . Available: https://www.flowmeters.com/thermal-technology
- [5] Universal Flow Monitors, Inc., "Differential Pressure Flowmeter Technology", flowmeters.com . Available: https://www.flowmeters.com/differential-pressure-technology
- [6] ANSI/AMCA Standard 210-16 / ANSI/ASHRAE Standard 51-16, "Laboratory Methods of Testing Fans for Certified Aerodynamic Performance Rating", Air Movement and Control Association International, Arlington Heights, IL, and American Society of Heating, Refrigerating and Air-Conditioning Engineers, Atlanta, GA, 2016.
- [7] E. Neese, "Understanding and Applying the 3 Basic Fan Laws", eldridgeusa.com, September 4, 2019. [Online]. Available: https://eldridgeusa.com/blog/understanding-and-applying-the-3-basic-fan-laws/
- [8] S.L. Dixon, C.A. Hall, "Fluid Mechanics and Thermodynamics of Turbomachinery (Sixth Edition) Chapter 5 Axial-Flow Compressors and Ducted Fans, Butterworth-Heinemann", 2010, Pages 143-181
- [9] A. Eleftherios, "Design of a low speed vaneaxial fan", 2011.
- [10] Delta Electronics, Inc., "Delta DC fan ASB0512MBEHD datasheet", 2018.

- [11] Automotive Electronics Council (AEC), "AEC Q100: Failure Mechanism Based Stress Test Qualification For Integrated Circuits", 2023. [Online]. Available: http://www.aecouncil.com/AECDocuments.html
- [12] Automotive Electronics Council (AEC), "AEC Q200: Stress Test Qualification For Passive Components", 2023. [Online]. Available: http://www.aecouncil.com/AECDocuments.html
- [13] J.E. Hrisko, "The Design and Characterization of a 3D Printed Venturi Tube", Maker Portal, 2020. Available: https://makersportal.com/.
- [14] International Organization for Standardization, "ISO 5167-4:2003: Measurement of fluid flow by means of pressure differential devices inserted in circular cross-section conduits running full Part 4: Venturi tubes", Ed.1, 2003.
- [15] American Society of Mechanical Engineers, "Flow Measurement PTC 19.5 2004. American Society of Mechanical Engineers", 2004.
- [16] https://ansyshelp.ansys.com/
- [17] Sensirion AG, "Datasheet SDP8xx-Digital", SDP810-500Pa, Version 1.1, 2019.
- [18] Sensirion AG, "Datasheet SHT85", SHT85, Version 4, 2021.
- [19] Patel, Sagar, PrachiTalati, and Saniya Gandhi. "Design of I2C protocol." International Journal of Technical Innovation in Modern Engineering Science 5.03 (2019): 741-74.
- [20] Philips Semiconductors, "The I2C-bus specification", Version 2.1, 2001.

Acknowledgements